UNIVERSITY OF CALIFORNIA
RIVERSIDE

Ausforming and Tempering of a Computationally Designed Ultra-High Strength Steel

A Thesis submitted in partial satisfaction
of the requirements for the degree of

Master of Science

in

Mechanical Engineering

by

Johny Quan

September 2018

Thesis Committee:
Dr. Suveen N. Mathaudhu, Chairperson
Dr. Masaru P. Rao
Dr. Peter A. Greaney

The Thesis of Johny Quan is approved:

_____

_____

_____

Committee Chairperson

University of California, Riverside

Acknowledgements

The research work of this thesis was carried out at the Mathaudhu Research Lab, Pacific Northwest National Laboratory (PNNL) and Central Facility for Advanced Microscopy and Microanalysis (CFAMM) at the University of California, Riverside. The research was funded by QuesTek Innovations LLC under the Small Business Innovative Research (SBIR) project "Adaptation of Ferrium M54 for Personal Armor."

This research work would not have been possible without the support of many these past two years. I would like to acknowledge and thank:

- Dr. Suveen Mathaudhu for not only serving as my advisor, but for guiding my research and fostering my passion for materials science and superheroes. It has been such a huge blessing to learn from you these past four years since ME 114. I also thank you for your patience with me when I would be off skydiving or staying up all night watching Luke Cage when I should have been in the lab or getting rest for a full day of work at PNNL. I look forward to many more years of friendship with you, Alicia, Leia and Maya.
- Dr. Thomas Kozmel from QuesTek for providing the opportunity to work on such an exciting project and providing technical expertise these past two years. It has been a great pleasure collaborating on such a fun project and learning from you.
- Christian Roach and Sina Shahrezaei for always being willing to help me in the lab with any issue or problem that I encountered. I would have done very little research and accomplished even less without both of your technical support and expertise. Almost every skill and technique that I've learned these past four years in the Mathaudhu Lab was from you two including sample preparation, metallography,

mechanical testing, machining, rolling, etc., etc. To the both of you, I wish you all the best. P.S. Don't be surprised if I continue calling you guys for help when I run into future problems ;).

- Darrell Herling and Karl Mattlin who made all of the full-scale trials at PNNL possible and successful. Without their expertise, willingness to work during a snowstorm and push their rolling mill to its operational capacity, half of this thesis work would not have been possible.
- Matt McCormick and Steve Rightnar for machining all my rolling samples, armor plates and tensile samples for me in the machine shop at UCR. I apologize for all the damages that I've inflicted upon your machinery while trying to machine my ultra-high strength materials! Thank you, Matt, for coming in early to help me machine samples, encouraging me and reassuring me that everything is going to work out and be okay! Thank you, Steve, for your attention to detail while cutting all of my tapered samples and tensile test samples. I owe you both a great deal of thanks for your enormous contributions.
- Dr. Yiwei Sun for all the help that you've provided me in such a short amount of time. I would not be very far at all in writing this thesis right now if you had not joined our group as a postdoctoral researcher and helped me with sample preparation, microscopy, technical writing, etc..
- Everyone at the Mathaudhu Lab who helped me with sample preparation (Loh and Lauren), stayed up late with me to perform late night ausforming trials (Heather, Jocelyn, Lauren, Jonathan) and labored with me for hours trying to get good mechanical testing data (Martin, Sina, Christian). It has been such a wild ride these

past few years and I am so very grateful and indebted to each of you for your friendship and all the help and support you all have given me.

- My big brothers, Kevin and William, for being amazing role models in my life. Kevin, your passion and joy in working for the Lord have encouraged me to have that same attitude in my own work. William, thank you for always believing in me, even from the very beginning and coming to tutor me for my first engineering exams during my freshman year of college when I was doing so poorly.
- My parents, Wilson and Lannie Quan, for sacrificing every form of earthly comfort imaginable to provide me with the opportunity to learn and experience the most wonderful life that I could ever ask for. Thank you for always believing the best in me, for visiting often to bring me homecooked meals and for bringing Dappy along as well to cheer me up and make me happy.
- My beloved wife and best friend Alicia, for helping me through this past year of graduate school. I thank you for your sacrificial love and patience during those late nights of experiments and when I would bring my stress and frustration home from school (which was often). You are the greatest treasure that God has brought to me during this season of my life (Proverbs 31:10-11). I am honored to be your husband.
- My Great Savior and King, Jesus Christ. Thank you for blessing me with the opportunity to work with and learn from so many amazing people. Thank you for the work that You've done and continue to do in my heart despite my total and utter depravity. I am truly undeserving of such amazing grace, mercy and blessing. Thank you for comforting me all those times I was ready to give up. Thank you for saving my dad. Thank you for loving me and being with me always, especially at school and in the lab. To the King eternal, the only God, be honor and glory forever and ever. Amen.

Dedication

It is to my late father, Wilson Quan, that this thesis is dedicated. I look forward to that future day described in Revelation 19:6-9 and 1 Thessalonians 4:13-18 when we are reunited together in glory with our Savior King. I can't wait to sing some of the same songs that we sung together when I held your hand as you took your last breath here on earth and took your first breaths with the Good Shepherd.

Psalm 23

The Lord is my shepherd,

I shall not want.

He makes me lie down in green pastures;

He leads me beside quiet waters.

He restores my soul;

He guides me in the paths of righteousness

For His name's sake.

Even though I walk through the valley of the shadow of death,

I fear no evil, for You are with me;

Your rod and Your staff, they comfort me.

You prepare a table before me in the presence of my enemies;

You have anointed my head with oil;

My cup overflows.

Surely goodness and lovingkindness will follow me all the days of my life,

And I will dwell in the house of the Lord forever.

ABSTRACT OF THE THESIS

Ausforming and Tempering of a Computationally Designed Ultra-High Strength Steel

by

Johny Quan

Master of Science, Graduate Program in Mechanical Engineering
University of California, Riverside, September 2018
Dr. Suveen Mathaudhu, Chairperson

Ferrium® M54® is a computationally designed ultra-high strength (UHS) steel with the potential for achieving outstanding strength, ductility, toughness and stress corrosion cracking resistance. M54 steel is currently being used in demanding areas, such as aerospace, defense, energy and construction, where high strength and toughness is needed while operating in extreme environments. Critical to the properties and performance of M54 steel is its hierarchical lath martensite microstructure which is further strengthened by finely dispersed, nanoscale carbide precipitates. In this study, a novel thermomechanical controlled processing (TMCP) technique, ausforming, was investigated to reveal the relationships between processing, microstructure and mechanical properties of M54 and improve its performance. Ausforming was shown to be an effective way to significantly refine the martensitic microstructure and further enhance the properties of the novel UHS steel products. In addition, ausforming also proved to accelerate the age hardening behavior and reduced the necessary heat treatment time. Ausforming was performed via single pass, high reduction warm rolling in the current study with both pilot-scale and full-scale trials.

The effect of ausforming parameters on microstructure and mechanical properties was investigated and the ausforming parameters were optimized. The processability and scalability of the ausforming process were also discussed. Subsequent to ausforming, isothermal tempering studies were conducted to look into the effects of severe ausforming on M_2C carbide precipitation in M54. The combined effects of microstructural refinement and nanoprecipitate strengthening maximized the combination of strength and ductility.

Table of Contents

Nomenclature

AF	As-Ausformed
APT	Atom Probe Tomography
AT	Ausformed and Tempered
AQ	As-Quenched
CBS	Concentric Backscattered
DSC	Differential Scanning Calorimetry
EBSD	Electron Backscattered Detection
EDM	Electrical Discharge Machining
ECAP	Equal Channel Angular Pressing
EL	Elongation
Fe_3C	Cementite
HRC	Rockwell C Hardness
HR-TEM	High Resolution Transmission Electron Microscopy
HTT	High Temperature Tempering
HV 1kg	Vickers Hardness with 1 kg Load
IRM	International Rolling Mills
K_{1C}	Fracture Toughness
K_{1SCC}	Stress Corrosion Cracking Resistance
ITT	Intermediate Temperature Tempering
LM	Light Microscopy
ND	Normal Direction

PAG	Prior Austenite Grain
PH	Precipitation Hardening
PNNL	Pacific Northwest National Laboratory
QT	Quench and Temper
RD	Rolling Direction
RT	Room Temperature
SEM	Scanning Electron Microscopy
SH-HA	Secondary Hardening High Alloy
TD	Transverse Direction
TEM	Transmission Electron Microscopy
TMCP	Thermomechanical Controlled Processing
UHS	Ultra-High Strength
UTS	Ultimate Tensile Strength
wt%	Weight Percent
XRD	X-Ray Diffraction
YS	Yield Strength

List of Figures

List of Tables

Chapter 1. General Introduction

1.1 Motivation

Since the 1940s, the increasing need for stronger and tougher materials in demanding areas, such as aerospace, defense, energy and construction has led to the development of ultra-high strength (UHS) steels possessing tensile strengths greater than 1400 MPa like maraging steels, precipitation hardening (PH) steels, low alloy steels and secondary hardening high alloy (SH-HA) steels [1]. In the 1960s, the need for improved fracture toughness and resistance to stress-corrosion cracking in submarine hull and aircraft steels resulted in the sponsored research of SH-HA steels by the U.S. Air Force and the development of AF 1410 in the late 1970s [2]. Since then, SH-HA steel compositions were continually optimized and improved, causing the Aermet steels to emerge in the 1990s followed by the rapid development and commercialization of the Ferrium steels in recent years from 2008 to 2012.

Secondary hardening high alloy (SH-HA) steels possess a unique balance of ultra-high strength and good ductility through their hierarchical lath martensitic microstructures with finely dispersed, coherent M_2C carbide precipitates (M = Mo, Cr, W, V) [3, 4, 5]. Over the last 50 years, optimized alloy compositions and processing conditions have led to continual strength and toughness improvements in SH-HA steels. However, to achieve these exceptional strength and toughness levels, an extended tempering process at elevated temperature is required for the precipitation of the nanoscale M_2C carbides [6, 7]. This

conventional quench and temper (QT) process can potentially consume a significant amount of time, energy and money.

An alternative approach that may improve both the mechanical properties of SH-HA steels as well as the development cycle time is the thermomechanical controlled processing (TMCP) method: ausforming (Fig 1.1). During ausforming, the UHS steel is cooled to the non-recrystallization temperature region after austenitization where it is plastically deformed before quenching to obtain a work-hardened lath martensite microstructure [8].

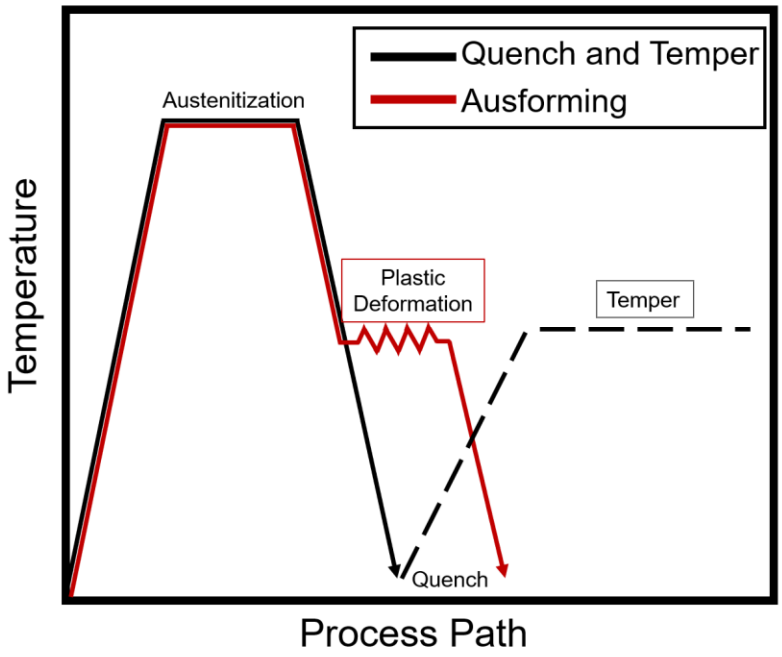

Fig. 1.1 Process paths for ausforming and the conventional quench and temper (QT) treatment.

This process leads to increased dislocation density and significant refinement of the hierarchical martensitic microstructure which further enhances the strength, toughness as well as the tempering response compared to the QT condition [9, 10].

Recently, laboratory studies have shown the ausforming process to be an effective strengthening method for UHS steels by microstructural refinement and work hardening of the packet/block/lath microstructure. For example, Gibbons performed UHS steel ausforming via high temperature equal-channel angular pressing (ECAP) to reduce the prior austenite grain (PAG) size from 188 μm to 14.8 μm which produced an increase in yield strength and ultimate tensile strength from 1360 MPa and 1730 MPa to 1680 MPa and 1980 MPa, respectively [11]. Kimura also studied the effects of ausforming on the strength and toughness of UHS steel. After 74% ausforming via multi-pass rolling, the yield strength and ultimate tensile strength increased from 1330 MPa and 1570 MPa to 1540 MPa and 1740 MPa, respectively, without loss in ductility [12]. The results of these studies are promising but the high flow stress of modern SH-HA steels has made it challenging to investigate and report on the commercial scalability and processability of ausforming with full-scale samples of SH-HA steel.

There are also some studies that show the improved secondary hardening response of ausformed SH-HA steels during tempering. Cho observed that lower deformation temperatures improved the degree of secondary hardening as well as accelerated the secondary hardening peak due to the increased density of dislocations and stored strain energy [13]. The peak aged sample that was ausformed at 600°C for 1 hour had a tensile strength of 2340 MPa compared to the non-ausformed sample which reached its peak hardness and tensile strength of 58 HRC and 2225 MPa, respectively, at 10 hours.

This thesis aims to further understand the fundamental processing-microstructure-properties relationships of UHS steel ausforming and to investigate the potential of ausforming to maximize the strength and toughness of the recently commercialized SH-HA steel, Ferrium® M54®. This thesis work will be divided into three chapters:

Chapter 1 will include a brief overview of ultra-high strength (UHS) steels and Questek's computationally designed SH-HA steel: Ferrium® M54® (hereafter referred to as "M54 steel"). A general review will also be given regarding to the processing, microstructure and properties of QT UHS steels and ausformed UHS steels.

Chapter 2 will focus on investigating the processing-microstructure-properties relationships of M54 steel ausforming. The effects of rolling reduction (%) and deformation temperature (°C) on the microstructure and properties of M54® steel will be discussed. Scalability of ausforming will also be tested by comparing the microstructure and properties of pilot-scale M54 coupons with full-scale M54 plates.

Chapter 3 will focus on understanding the secondary hardening behavior of ausformed M54 steel during tempering. The combination of ausforming and tempering has been shown to produce work-hardened/refined lath martensite with dispersed M_2C carbides. The effects of ausforming will be explored by tempering ausformed M54 steel at 350°C, 425°C and 516°C. The processing-microstructure-properties relationships of the ausformed and peak tempered condition will be compared with the conventional QT condition.

1.2 Ultra-High Strength Steels

UHS steels are a family of advanced steel alloys with tensile strengths greater than 1400 MPa that includes maraging steels, precipitation hardening (PH) stainless steels, low alloy steels and secondary hardening high alloy (SH-HA) steels. Fig. 1.2 shows possible applications for these steels which include armor, aircraft landing gear, rotor shafts, drive shafts and many more.

Fig. 1.2 Examples of UHS steel applications that require high specific strength and toughness include personal armor, aircraft and vehicular components [14].

These steels are classified by their alloy compositions, thermal processing and characteristic microstructures. UHS steels differ in alloy composition but they all possess a lath martensitic microstructure strengthened by nanoscale precipitates which will be further introduced in sections. Table 1.1 shows the typical alloying elements used in various UHS steels which include nickel (Ni), cobalt (Co), chromium (Cr), molybdenum (Mo), manganese (Mn), vanadium (V) and more [18, 19, 20]. The various combinations of

these alloy additions play a major role on the processability, microstructure and resulting properties in UHS steels. For example, 300M alloy is strengthened by the formation of ε-carbides during tempering while Maraging 250 is strengthened by Ni_3Ti and Fe_2Mo intermetallic precipitates because of it's Fe, Ni, Ti and Mo alloy combination [7, 15]. SH-HA steels like Aermet 100 and Ferrium® M54® include additions of Cr, Mo and V which are known to be strong M_2C carbide formers during tempering [16]. These different alloying combinations play important roles in UHS steels regarding lath martensite formation, dislocation density, precipitation hardening and many more [6, 17].

Table 1.1 Compositions of UHS steels used in aerospace applications [18, 19, 20].

Alloy	C	Ni	Co	Cr	Mo	Mn	V	W	Si	Al	Ti	S	P
HP 9-4-20	0.2	9	4	0.8	1	0.1-0.3	0.08	—	0.2	—	—	—	—
HY 180	0.1	10	8	2	1	0.15	—	—	—	—	—	—	—
AF 1410	0.16	10	14	2	1	—	—	—	—	—	—	—	—
Maraging 250	0.03	17-19	7.0-0.85		4.6-5.1	0.01	—	—	0.1	0.05-0.15	0.3-0.5	0.01	0.01
4340	0.4	1.8	—	0.85	0.25	0.7	—	—	1.6	—	—	—	—
300M	0.4	1.8	—	0.85	0.4	0.7	0.1	—	1.6	—	—	—	—
Aermet 100	0.23	11.1	13.4	3.1	1.2	—	—	—	—	—	0.05	—	—
Ferrium S53	0.21	5.5	14	10	2	—	0.3	1	—	—	—	—	—
Ferrium M54	0.3	10	7	1	2	—	0.1	1.3	—	—	—	—	—

As Table 1.1 shows, different UHS steels can vary significantly in chemical composition. Each composition will require a unique heat treatment schedule in order to achieve the desired microstructure and properties. Different applications will require certain UHS steels to be used over others depending on the required properties and operating conditions. The need for tougher UHS steels in highly stressed structural components operating under extreme environmental conditions led to the development of SH-HA steels in the 1960s. This particular class of UHS steels maximizes strength, toughness and environmental

fatigue resistance by utilizing alloy additions greater than 10 wt% that include strong carbide forming elements which results in a hierarchical lath martensitic microstructure with finely dispersed, nanoscale M_2C carbide precipitates after a quench and temper (QT) heat treatment. The term "secondary hardening" refers to the hardness increase that is associated with the M_2C carbide precipitation during tempering.

Optimized alloy compositions, processing conditions and heat treatment schedules have led to notable strength and toughness improvements in SH-HA steels over the last 50 years from AF1410 (1970s) and Aermet 100 (1990s) to Questek's recently commercialized alloy, Ferrium® M54® (2011). QuesTek Innovations used their computational "Materials by Design" approach to efficiently develop and commercialize a new SH-HA steel with reduced Co content, Ferrium® M54®, which surpasses the current standard, Aermet 100, in terms of cost-effectiveness and performance. Fig. 1.3 compares various UHS steels like 300M, Maraging, Aermet 100, Ferrium® M54® steel and some of their most critical structural properties like ultimate tensile strength (UTS), fracture toughness (K_{1C}) and stress corrosion cracking resistance (K_{1SCC}). 300M steel is a low alloy UHS steel that was commonly used for several decades in extreme structural applications such as aircraft landing gear and airframe parts, however, it's fracture toughness and stress corrosion cracking resistance needed to be improved to ensure safety and longevity [21]. Recently developed SH-HA steels like Aermet 100 and Ferrium® M54® are more suitable for applications in extreme environments such as naval aircraft landing gear.

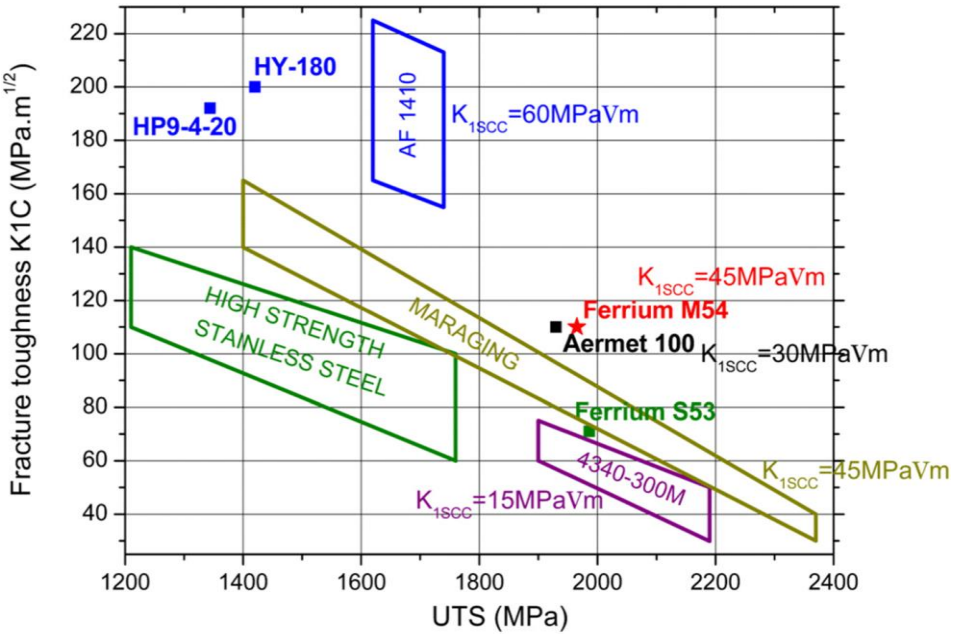

Fig. 1.3 Ultimate tensile strength (UTS), fracture toughness (K_{1C}), and stress corrosion cracking resistance (K_{1SCC}) of various UHS steels. [21]

The continual development of UHS steel alloys demonstrates how understanding the fundamental processing-microstructure-properties relationships of these complex martensitic alloys is the key to meeting future design goals such as improving strength, toughness, weight savings, energy efficiency and production costs.

1.3 Martensite in Steel

Martensite is known to be the strongest form of steel which forms when austenite is rapidly cooled (quenched) from high temperature. The rapid cooling prevents carbon atom diffusion, producing high shear strain and a distorted lattice due to the trapped carbon. Martensite crystals form at the speed of sound during quenching in order to minimize the strain energy caused by carbon supersaturation. Therefore, the martensitic transformation

is described as a diffusion-less, shear-type phase transformation. It is now understood that the martensitic transformation can result in either a lath or plate morphology depending on the carbon content. The details of both lath and plate martensite formation are clearly discussed in existing literature [22, 23, 24, 25, 26, 27, 28]. Both plate and lath martensite will be introduced, however, the focus in this thesis will be on lath martensite because UHS steels, specifically SH-HA steels, are all low to medium carbon steels (< 0.60 wt%) which possess lath martensite microstructures.

As shown in Fig. 1.4, low to medium carbon steels ($0 \leq 0.60$ wt%) will form a lath martensite microstructure which is composed of highly ordered packets, blocks and laths within a prior austenite grain (PAG) while higher carbon steels (> 0.60 wt%) will form a plate martensite microstructure where plates composed of finely spaced transformation twins are the dominant structures [24]. The fraction of retained austenite also continually increases with higher carbon content. The distinctive features of these morphologies play a major role on the strength and toughness of martensite.

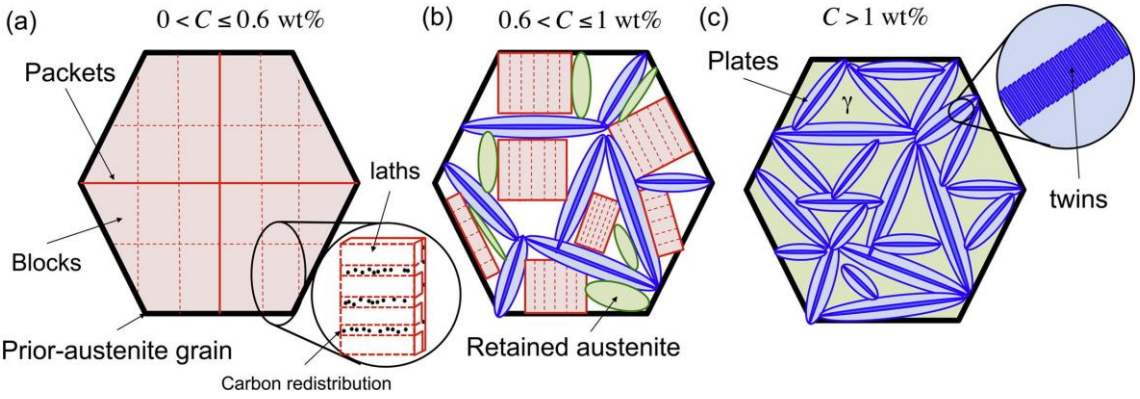

Fig. 1.4 (a) Hierarchical lath martensite microstructure formed in low to medium carbon steels (< 0.60 wt%). (b) Mixed structure containing plates, retained austenite and packet structures formed in higher carbon steels (0.60 < C ≤ 1 wt%) (c) Plate martensite structure dominated by plates with twins and a considerable fraction of retained austenite formed in high carbon steels (C > 1wt%). [24].

Lath martensite has a hierarchically ordered microstructure containing parallel arrays of lath-shaped crystals, while plate martensite has non-parallel arrays of plate-shaped crystals without hierarchical order and can be mixed with dislocation arrays and retained austenite [22, 24, 29]. High carbon steels (0.6 < C ≤ 1 wt%) with mixed plate structures, dislocation arrays and retained austenite have significantly higher hardness levels than low carbon steel but they are also brittle due to microcracks caused by the randomly oriented plates impinging one another during quenching [22]. In the case of ultra-high carbon steels (C > 1 wt%), the higher fraction of retained austenite leads to decreased hardness but improved ductility.

The hierarchical, building block microstructure of lath martensite is composed of packets, blocks and nano-sized laths within a prior austenite grain (PAG). These fundamental microstructural units have been observed to control the mechanical properties of UHS steels, especially the toughness [30].

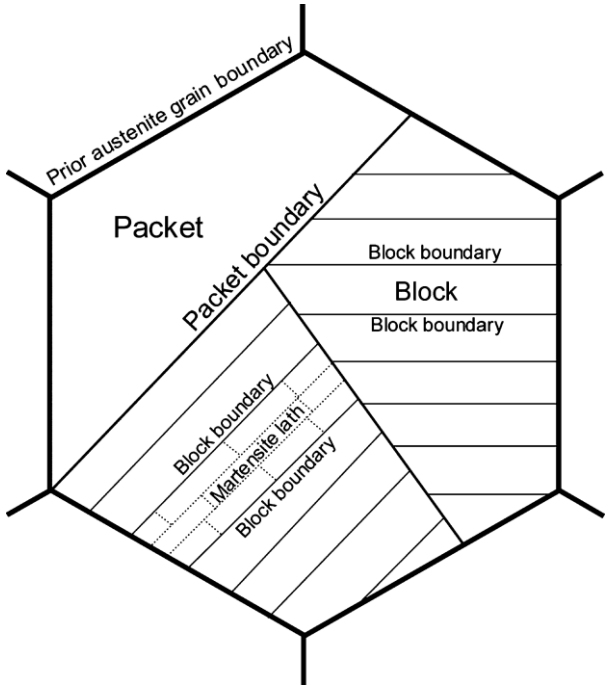

Fig. 1.5 Hierarchical microstructure of lath martensite within a single prior austenite grain composed of packets, blocks and laths [23]

There are many high and low angle boundaries that separate the different microstructural units as shown in Fig. 1.5 [23]. The boundaries that separate the PAGs, packets and block arrays are high angle (>15°) while the boundaries between individual blocks in a packet and laths in a block are low angle (<15°). High angle boundaries have been shown to be effective in blocking dislocation motion which is why the parallel lath martensite microstructure possesses higher much higher toughness than the non-parallel plate martensite microstructure. However, due to it's crystallographic complexity and nanoscale dimensions, comprehensive characterization of lath martensite can be challenging and would require electron backscattered diffraction (EBSD) analysis with high resolution as well as transmission electron microscopy (TEM).

1.4 Tempering of Lath Martensite in Ultra-High Strength Steels

In addition to having hierarchical lath martensite microstructures, UHS steels are also strengthened by finely dispersed nanoscale precipitates that are formed during tempering. Table 1.2 shows that the tempering duration may last between 5 to 12 hours depending on the type of UHS steel, part size and desired balance of strength and ductility [1, 4, 30]. As mentioned in Section 1.2, depending on the alloy composition, these precipitates can either be intermetallic compounds or alloy carbides. SH-HA steels, which contain strong carbide forming elements, are strengthened by M_2C carbides after extended tempering. The formation of these M_2C carbides can further increase tensile strength levels to above 2000 MPa. These M_2C carbide precipitates also improve ductility, because they preferably nucleate at dislocations and are finely dispersed throughout the laths.

Table 1.2 Mechanical properties of several UHS steels and the required tempering treatment in order to obtain balance of ultrahigh strength and toughness [1, 4, 31].

	YS (MPa)	UTS (MPa)	Elongation (%)	Temper Temperature (°C)	Temper duration (h)
Ferrium M54	1730	2020	15	515	10
Aermet 100	1723	1965	13	482	5
Maraging 250	1723	1827	12	482	6
AF 1410	1544	1680	17	510	5
Ferrium S53	1470	1990	15	482	12
HP 9-4-20	1345	1480	14	540 - 565	4 - 8
HY - 180	1207	1310	12	482 - 510	5 - 10

Although the conventional QT approach has led to great improvements in strength and toughness, it can also greatly increase energy consumption, processing time and cost from a practical manufacturing standpoint.

1.5 Thermomechanical Controlled Processing

An alternative strengthening approach that can be used to obtain this combination of strength and toughness in martensitic steels without the need for an extended tempering treatment is thermomechanical controlled processing (TMCP). TMCP combines heat treatment, controlled rolling and accelerated cooling in order to control and refine the various microstructures of steel as shown in Figure 1.6 [32].

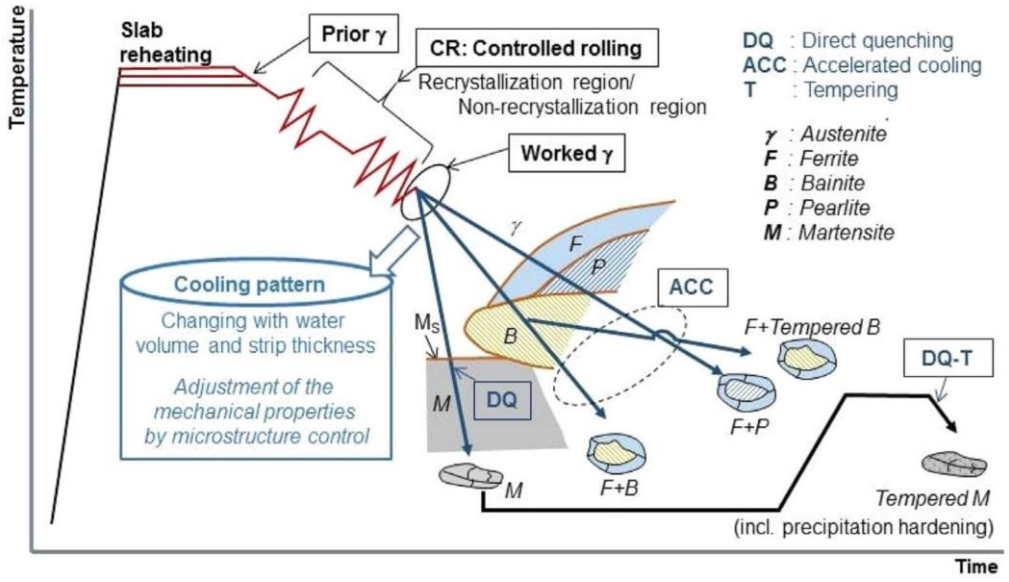

Fig. 1.6 Different thermomechanical controlled processing (TMCP) paths to achieve a variety of refined and work-hardened steel microstructures [32]

During controlled rolling, the steel can be plastically deformed in the recrystallization and non-recrystallization temperature regions to produce a pancaked and work hardened

austenite microstructure prior to cooling. Different cooling patterns and tempering process paths open up possibilities for a variety of refined microstructures with enhanced mechanical properties. The advancement of TMCP with controlled rolling has led to finer and finer grained structural steels with improved mechanical properties in the last century. Industrial steel plate manufacturers have incorporated microalloying and TMCP to produce stronger and tougher steels by controlling the microstructures of their rolled products [32]. If the industrial trend continues towards TMCP of stronger and tougher materials such as UHS steels, it becomes even more pertinent to further investigate the processing-microstructure-properties relationships and scalability of TMCP methods for martensitic steels.

1.6 Ausforming of Ultrahigh Strength Steel

Studies have shown the TMCP method, ausforming, to be an effective strengthening method for lath martensitic UHS steels [33, 34, 35, 36]. During ausforming, UHS steel is cooled to the non-recrystallization temperature region after austenitization where metastable austenite is plastically deformed before martensitic transformation during direct quenching (Fig. 1.7).

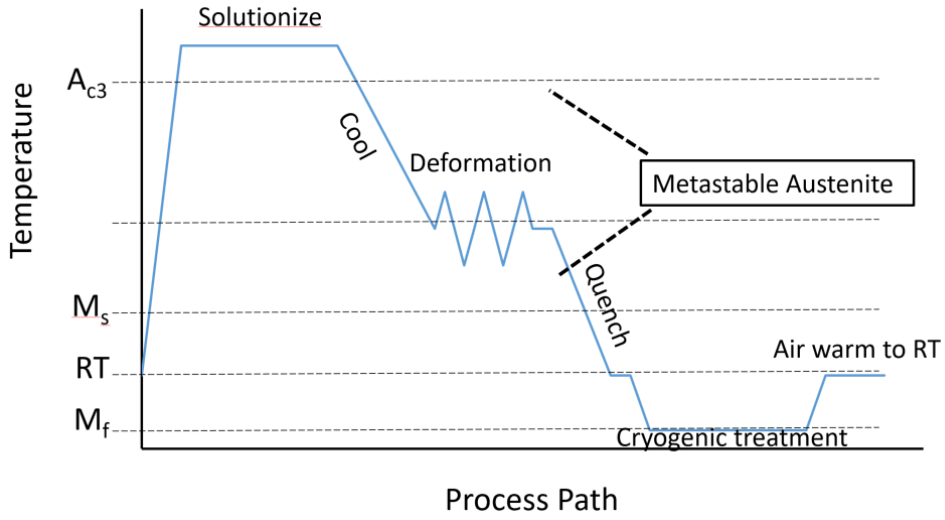

Fig. 1.7 Ausforming process path

Alloying elements such as nickel (Ni), molybdenum (Mo) and chromium (Cr) are austenite stabilizers that allow for longer transformation time of metastable austenite before secondary phases like pearlite and bainite start to form. This makes secondary hardening UHS steels promising candidates for ausforming due to their high alloy content that includes Ni, Co and Cr [6].

Ausforming leads to significant microstructural refinement because a high density of dislocations can accumulate within the work-hardened metastable austenite at lower temperatures [10]. The dislocations and sub-grain boundaries serve as nucleation sites for martensite, thus reducing the packet and block size [13]. During direct quenching, the accumulation of dislocations is inherited into the lath martensite microstructure leading to refinement of the packets, blocks and laths [10]. The packet and block boundaries are also favorable for ductility because they are high angle and act as barriers to moving dislocations [37]. In addition to increasing the strength of as-quenched lath martensite, the

high dislocation density and large stored strain energy in the pancaked austenite grains can possibly improve the secondary hardening response during tempering [10]. The ausforming process needs to be carefully controlled in order to obtain increased strength without adverse effect on ductility and toughness. By studying and developing the processing-microstructure-properties relationships of lath martensite ausforming, SH-HA steels can be better understood, and ausforming as a novel technique can be developed to obtain better structural materials.

This thesis investigates a novel TMCP route including ausforming and tempering to maximize strength and toughness beyond the conventional QT condition. The scalability of the process is also demonstrated by carrying out both pilot-scale ausforming and full-scale ausforming. The goal is to develop a better understanding of the processing-microstructure-properties relationship of the ausformed M54 steel as well as optimize the processing parameters, which will be beneficial to both the scientific community as well as the modern steel rolling industry.

References

[1] N. E. Prasad and R. J. H. Wanhill, "Aerospace Materials and Material Technologies SpringerLink." 2017. [Online]. Available: https://link.springer.com/content/pdf/10.1007/978-981-10-2134-3.pdf.

[2] ASM International, "Development of AF 1410 ultrahigh-strength steel." 13-Mar-2018.

[3] G. R. Speich, "Secondary Hardening Ultrahigh-Strength Steels," Innovations in Ultrahigh Strength Steel Technology, pp. 89–112, 1990.

[4] K. K. Sankaran and R. S. Mishra, Metallurgy and Design of Alloys with Hierarchical Microstructures. Elsevier, 2017.

[5] E. I. Galindo-Nava and P. E. J. Rivera-Díaz-del-Castillo, "A model for the microstructure behaviour and strength evolution in lath martensite," Acta Mater., vol. 98, pp. 81–93, Oct. 2015.

[6] J. H. Graves, "Effect of Heat Treatment on the Microstructure and Properties of AerMet (tm) 100 Steel," Worcester Polytechnic Institute, 1994.

[7] H. J. Kong and C. T. Liu, "A Review on Nano-Scale Precipitation in Steels," Technologies, vol. 6, no. 1, p. 36, Mar. 2018.

[8] T. V. Rajan, C. P. Sharma, and A. Sharma, Heat Treatment: Principles and Techniques. PHI Learning Pvt. Ltd., 2011.

[9] I. Tamura, "Some Fundamental Steps in Thermomechanical Processing of Steels," Transactions of the Iron and Steel Institute of Japan, vol. 27, no. 10, pp. 763–779, 1987.

[10] N. Tsuji and T. Maki, "Enhanced structural refinement by combining phase transformation and plastic deformation in steels," Scr. Mater., vol. 60, no. 12, pp. 1044–1049, Jun. 2009.

[11] S. L. Gibbons et al., "Microstructural refinement in an ultra-high strength martensitic steel via equal channel angular pressing," Materials Science and Engineering: A, vol. 725, pp. 57–64, May 2018.

[12] Y. Kimura and T. Inoue, "Combined Effect of Ausforming and Warm Tempforming on the Strength and Toughness of An Ultra-High Strength Steel," ISIJ Int., vol. 56, no. 11, pp. 2047–2056, 2016.

[13] K. S. Cho et al., "Influence of rolling temperature on the microstructure and mechanical properties of secondary hardening high Co–Ni steel bearing 0.28wt%

C," Materials Science and Engineering: A, vol. 527, no. 27, pp. 7286–7293, Oct. 2010.

[14] I. G. Crouch, "1 - Introduction to armour materials," in The Science of Armour Materials, Woodhead Publishing, 2017, pp. 1–54.

[15] Z. B. Jiao, J. H. Luan, M. K. Miller, Y. W. Chung, and C. T. Liu, "Co-precipitation of nanoscale particles in steels with ultra-high strength for a new era," Mater. Today, vol. 20, no. 3, pp. 142–154, Apr. 2017.

[16] E. U. Lee, R. Taylor, C. Lei and H. C. Sanders, "Aircraft Steels," NAWCAD Report No. NAWCADPAX/TR-2009/12, 19 Feb 2009.

[17] G. R. Speich, D. S. Dabkowski, and L. F. Porter, "Strength and toughness of Fe-10ni alloys containing C, Cr, Mo, and Co," Metallurgical Transactions, vol. 4, no. 1, pp. 303–315, Jan. 1973.

[18] W. M. Garrison, "Ultrahigh-strength steels for aerospace applications," JOM, vol. 42, no. 5, pp. 20–24, May 1990.

[19] J. M. Dahl, "New requirements for ferrous-base aerospace alloys," Aircraft Engineering and Aerospace Technology, vol. 73, no. 2, p. null, 2001.

[20] E. U. Lee, M. Stanley, B. Pregger, C. Lei and E. Lipnickas, "Ferrium M54 Steel," NAWCAD Report No. NAWCADPAX/TIM-2014/292, 2015.

[21] A. Mondiere, V. Déneux, N. Binot, and D. Delagnes, "Controlling the MC and M2C carbide precipitation in Ferrium® M54® steel to achieve optimum ultimate tensile strength/fracture toughness balance," Mater. Charact., vol. 140, pp. 103–112, Jun. 2018.

[22] G. Krauss, "Martensite in steel: strength and structure," Materials Science and Engineering: A, vol. 273–275, pp. 40–57, Dec. 1999.

[23] H. Kitahara, R. Ueji, N. Tsuji, and Y. Minamino, "Crystallographic features of lath martensite in low-carbon steel," Acta Mater., vol. 54, no. 5, pp. 1279–1288, Mar. 2006.

[24] E. I. Galindo-Nava and P. E. J. Rivera-Díaz-del-Castillo, "Understanding the factors controlling the hardness in martensitic steels," Scr. Mater., vol. 110, pp. 96–100, Jan. 2016.

[25] K. Iwashita, Y. Murata, Y. Tsukada, and T. Koyama, "Formation mechanism of the hierarchic structure in the lath martensite phase in steels," Philos. Mag., vol. 91, no. 35, pp. 4495–4513, Dec. 2011.

[26] S. Morito, H. Tanaka, R. Konishi, T. Furuhara, Maki, and T, "The morphology and crystallography of lath martensite in Fe-C alloys," Acta Mater., vol. 51, no. 6, pp. 1789–1799, 2003.

[27] S. Morito, H. Saito, T. Ogawa, T. Furuhara, and T. Maki, "Effect of Austenite Grain Size on the Morphology and Crystallography of Lath Martensite in Low Carbon Steels," ISIJ Int., vol. 45, no. 1, pp. 91–94, 2005.

[28] S. Morito, X. Huang, T. Furuhara, T. Maki, and N. Hansen, "The morphology and crystallography of lath martensite in alloy steels," Acta Mater., vol. 54, no. 19, pp. 5323–5331, Nov. 2006.

[29] A. Stormvinter, G. Miyamoto, T. Furuhara, P. Hedström, and A. Borgenstam, "Effect of carbon content on variant pairing of martensite in Fe–C alloys," Acta Mater., vol. 60, no. 20, pp. 7265–7274, Dec. 2012.

[30] S. Morito, H. Yoshida, T. Maki, and X. Huang, "Effect of block size on the strength of lath martensite in low carbon steels," Materials Science and Engineering: A, vol. 438–440, pp. 237–240, Nov. 2006.

[31] P. M. Novotny and T. J. McCaffrey, "An Advanced Alloy for Landing Gear and Aircraft Structural Applications-Aerometr® 100 Alloy," SAE Technical Paper, 1992.

[32] B. Buchmayr, "Thermomechanical Treatment of Steels - A Real Disruptive Technology Since Decades," Steel Res. Int., vol. 88, no. 10, p. 1700182, Oct. 2017.

[33] S. Morito, I. Kishida, and T. Maki, "Microstructure of ausformed lath martensite in 18% Ni maraging steel," in Journal de Physique IV (Proceedings), 2003, vol. 112, pp. 453–456.

[34] M. Seifert, M. Botzet, and W. Theisen, "Hardness and Microstructure of a Newly Developed Stainless Steel after Ausforming," Steel Res. Int., vol. 88, no. 10, p. 1700010, Oct. 2017.

[35] J. Hoffmann, M. Rieth, L. Commin, P. Fernández, and M. Roldán, "Improvement of reduced activation 9%Cr steels by ausforming," Nucl. Eng. Des./Fusion, vol. 6, pp. 12–17, Jan. 2016.

[36] Z. Li, X. Sun, Z. Yang, and Q. Yong, "Grain Refinement and Toughening of Low Carbon Low Alloy Martensitic Steel with Yield Strength 900 MPa Grade by Ausforming," in HSLA Steels 2015, Microalloying 2015 & Offshore Engineering Steels 2015, 2016, pp. 195–201.

[37] T. Furuhara, K. Kikumoto, H. Saito, T. Sekine, T. Ogawa, S. Morito & T. Maki, “Phase transformation from fine-grained austenite.” ISIJ international, 48(8), 1038-1045. 2008.

Chapter 2. Single Pass Ausforming of Ferrium® M54® steel

Abstract

Ferrium® M54® is a medium-carbon ultra-high strength steel with potential for achieving outstanding strength, toughness and stress corrosion cracking resistance. A processing route involving single pass ausforming at intermediate temperatures was investigated to reveal the relationships between processing, microstructure and mechanical properties. Pilot-scale ausforming was conducted via rolling at 550°C - 750°C with rolling reductions of 30% - 60%, and full-scale ausforming was performed at approximately 700°C with 45% reduction. Lath refinement of the martensitic microstructure was assessed via light microscopy, scanning electron microscopy and hardness testing. Tensile tests were performed on similarly processed pilot-scale and full-scale samples to evaluate the mechanical properties and test the scalability. The pilot-scale and full-scale 45% ausformed steels exhibited excellent mechanical properties with yield strengths of 1830 MPa and 1747 MPa, ultimate tensile strengths of 2257 MPa and 2291 MPa and total elongations of 14.4% and 13.4%, respectively. Ausforming has proven to be an effective way to highly-refine the martensitic microstructure and further enhance the performance of novel ultra-high strength steel products.

2.1 Introduction

Ausforming has the potential to achieve ultrahigh strength and excellent toughness in lath martensitic steels without the need for a subsequent tempering treatment. The ausforming process combines heat treatment, plastic deformation and martensitic transformation to achieve increased dislocation density and microstructural refinement [1, 2]. Ausforming of various UHS steels has been successfully demonstrated in the laboratory setting, but there are limited studies on modern SH-HA steels such as Ferrium M54 and none that investigate the scalability and processability of single pass ausforming with high reductions at lower temperatures to maximize microstructural refinement.

The processing-microstructure-properties relationships of lath martensitic UHS steels have been and continue to be a significant area of interest and research in metallurgy. Studies have shown that the size of the packets and blocks, which are separated by high angle boundaries, is directly related to the structural properties like strength, hardness and toughness [3, 4, 5]. A Hall-Petch relation exists between the strength of lath martensite and the size of its microstructural units [6, 7, 8]. Since the packet and block sizes correlate linearly with the prior austenite grain size (PAG), grain refinement of austenite prior to martensitic transformation can take advantage of the Hall-Petch relation to improve the balance of strength and toughness in lath martensitic steels by increasing the dislocation density and amount of high angle boundaries that act as barriers to dislocation motion [4, 9, 10].

Grain refinement of austenite has been achieved through heat treatments such as cyclic thermal processing and multiple austenitization treatments. Wang used cyclic treatment in

a commercial UHS steel, 17CrNiMo6, to refine the PAG size from 199 μm to 6 μm which increased the yield strength by 235 MPa and improved the Charpy U-notch impact energy more than 8 times [11]. However, these extended heat treatments may not be desirable due to time, energy and cost requirements. Grain refinement can also be achieved by the thermomechanical controlled processing (TMCP) technique, ausforming, where prior to martensitic transformation, austenite is cooled to and plastically deformed at lower temperatures where recrystallization would not occur. Ausforming can achieve significant microstructural refinement with higher dislocation density without the need for any additional thermal processing steps [12]. Fig. 2.1 shows the formation of lath martensite packets and blocks within a prior austenite grain during normal quenching versus ausforming [13]. The hierarchical structure of lath martensite forms to minimize the strain energy and eliminate the shear strain caused during the diffusionless shear transformation. Therefore, the increased stored strain energy due to severe ausforming allows more packets to form within a PAG, leading to finer lamellar block structures containing ultrafine and nanoscale substructures (sub-blocks, laths).

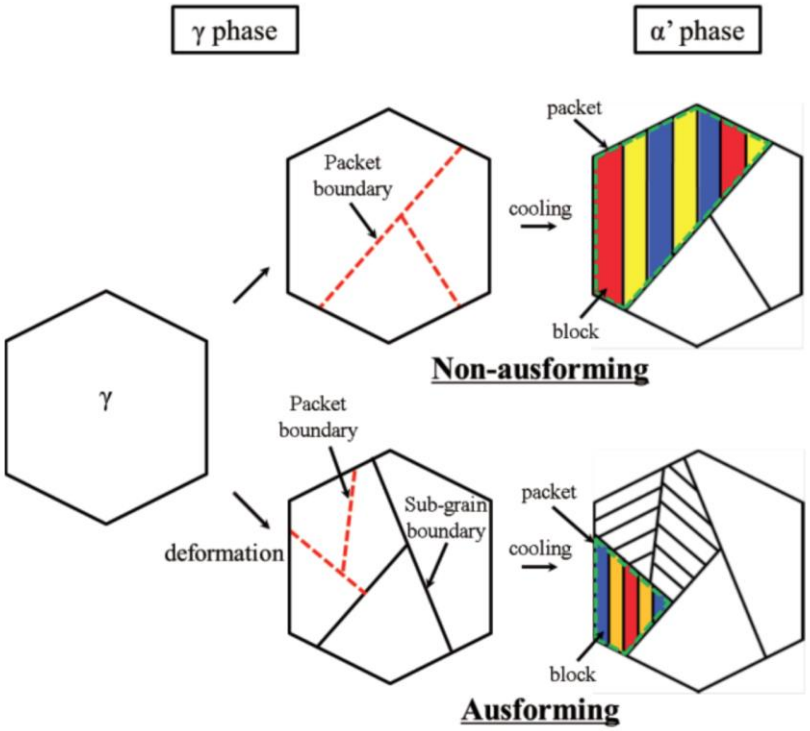

Fig. 2.1 Lath martensite formation in the non-ausformed and ausformed condition. Deformation causes more packets and finer blocks to form to accommodate increased strain [13].

Prior studies have shown that the amount of microstructural refinement can be controlled by the amount of strain applied during ausforming. Morito conducted ausforming of lath martensite in 18% Ni maraging steel with 20% and 60% rolling reduction at 500°C (Fig. 2.2) [14]. After 20% ausforming, the morphology was not so different from the non-ausformed condition, however, 60% ausforming resulted in an increased number of elongated packets with decreased block width within a prior austenite grain.

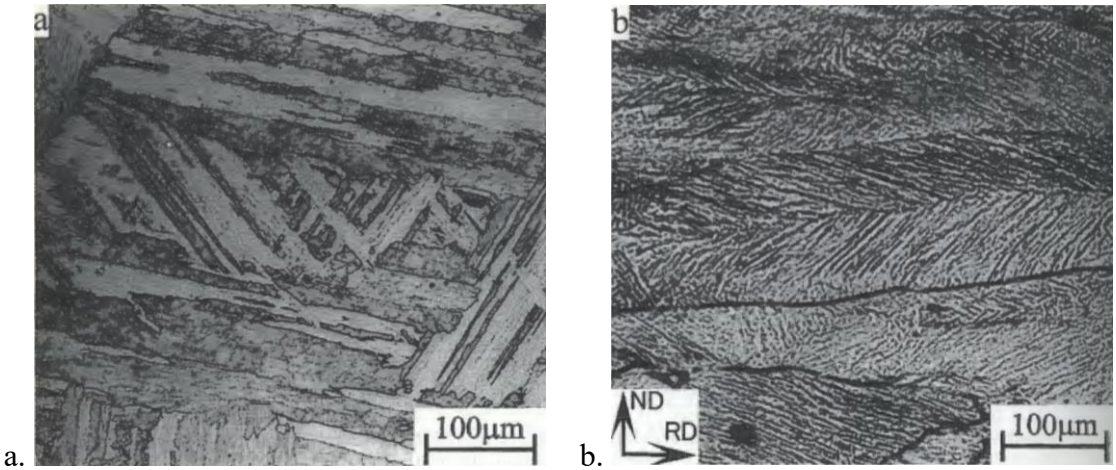

Fig. 2.2 Microstructure of lath martensite in 18% Ni maraging steel in the (a) non-ausformed condition and (b) after 60% ausforming reduction [14].

Table 2.1 shows that the packet, block and lath widths were all significantly reduced within the highly pancaked PAGs after 60% ausforming. The dislocation density is also higher since the dislocations generated during austenite deformation in the non-recrystallization temperature region are inherited into the lath martensite microstructure during quenching.

Table 2.1 Microstructural refinement of lath martensite in 18% Ni maraging steel after 60% ausforming [14].

Reduction	0%	60%
Packet width (um)	142	67
Block width (um)	18.6	2.5
Lath width (um)	0.80	0.64
Dislocation density ($10^{15}/m^2$)	0.91	1.30

Several other studies have investigated the effects of ausforming on the microstructure and properties of various UHS steels but there are very limited studies that have investigated

modern secondary hardening high alloy (SH-HA) steels containing Ni and Co such as Aermet 100 and Ferrium® M54®. These steels seem to be promising ausforming candidates due to their alloy composition which contains austenite stabilizers that allow for long metastable austenite transformation times before secondary phases start to form like ferrite and bainite.

In this study, various ausforming deformation temperatures and rolling reductions are tested to observe the effects on the microstructure and mechanical properties of Ferrium® M54® steel. A combination of light microscopy (LM), scanning electron microscopy (SEM), Vickers hardness and tensile testing is used to study the ausforming strengthening mechanisms. Scalability and processability of M54 steel ausforming was studied by comparing the results of pilot-scale coupons to full-scale plates. Single pass ausforming of pilot-scale coupons and full-scale plates was carried out at 550/650/750°C and 700°C, respectively. This resulted in elongated microstructures with pancaked PAGs in the rolling direction. After 30, 45 and 60% ausforming, the elongated PAG width of the pilot coupons were reduced from ~100 μm to ~60, ~50 and ~40 μm, respectively, at all deformation temperatures. After 30, 45 and 60% ausforming at 550°C, the block width decreased from 1.10 μm to 0.653, 0.471 and 0.240 μm. Signs of recovery and coarsening were observed in the full-scale samples that were rolled to 45% reduction between 500°C - 700°C.

Hardness increased linearly with higher rolling reduction and was consistent across all deformation temperatures, however, the full-scale sample with the coarsened microstructures and the pilot-scale samples that were 45% and 60% ausformed at 750°C showed slightly less hardness increases after ausforming. The 45% ausformed pilot-scale

and full-scale samples had yield strengths of 1830 MPa and 1747 MPa, ultimate tensile strengths of 2257 MPa and 2291 MPa and total elongations of 14.4% and 13.4%, respectively, which surpasses the yield and ultimate tensile strength of the conventional quench and tempered condition (1730MPa, 2020MPa) while maintaining good ductility. These results demonstrate the processability and scalability of single pass ausforming at intermediate temperatures (550°C - 750°C).

2.2 Materials and Methods

Raw Ferrium M54 steel was provided by QuesTek Innovations in the mill-annealed (normalized) condition for pilot scale and full scale ausforming studies. The chemical composition of M54 steel is shown in Table 2.2 [15].

Table 2.2 Ferrium M54 chemical composition (nominal wt. %) [15].

Fe	C	Co	Cr	Ni	Mo	W	V
Bal.	0.3	7	1	10	2	1.3	0.1

Pilot-scale coupons and full-scale plates of M54 steel were cut using wire electrical discharge machining (EDM) for single pass ausforming. The leading edges of the pilot-scale coupons were tapered according to the desired amount of rolling reduction as shown in Fig. 2.3. Nine pilot scale coupons were prepared to carry out the 30/45/60% ausforming reduction progression at 550/650/750°C. For the full-scale study, ten plates of M54 steel with dimensions 177.8 mm x 177.8 mm x 12.7mm were similarly tapered for 45% single pass ausforming at 700°C.

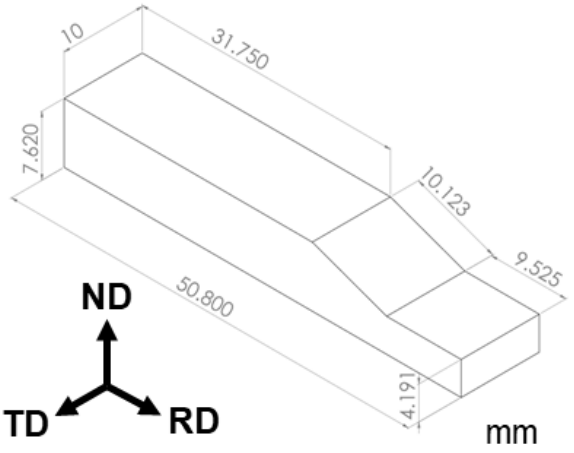

Fig. 2.3 Dimensions (mm) of a pilot-scale coupon with tapered edge for 45% single pass rolling. Rolling, transverse and normal directions are denoted by RD, TD and ND.

All of the pilot-scale coupons were ausformed at the University of California, Riverside in the Mathaudhu Research Lab using an International Rolling Mills (IRM) lab rolling mill (Model #4060) while the full-scale plates were ausformed at the Pacific Northwest National Laboratory (PNNL) using a Waterbury Farrel rolling mill. The IRM rolling mill speed was run at 2.06 in/min and the rollers were heated to 200°C to reduce heat loss during ausforming, while the Waterbury Farrel rolling mill did not have heating capabilities and was run at 2150 in/min to achieve single pass rolling of the full-scale plates.

The ausforming process path is depicted in Fig. 2.4 and is as follows: M54 steel coupons and plates were solution treated (austenitized) at 1060°C for 1 hour in a box furnace, air cooled to the deformation temperature for single pass rolling, quenched in an oil bath to room temperature, transferred to a liquid nitrogen bath for a 1 hour cryogenic treatment and air-warmed to room temperature before characterization.

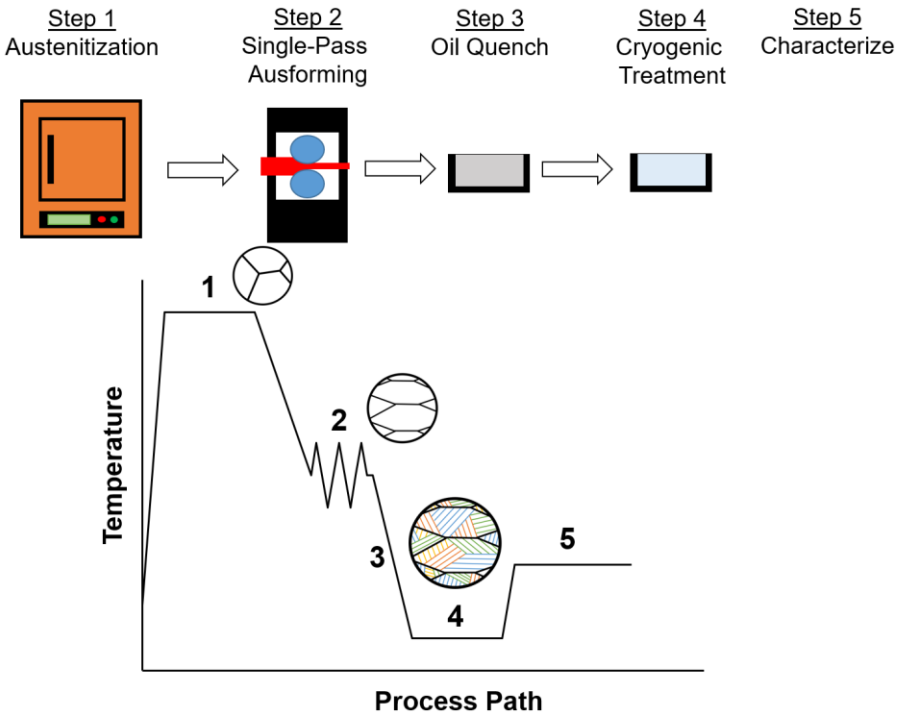

Fig. 2.4 Process path for single pass ausforming at reduced temperature.

Ausformed coupons and plates were sectioned along the longitudinal rolling direction (RD) for microstructural analysis and mechanical testing to compare with the conventional QT condition. The elongated microstructure illustrated in Fig. 2.4 on the plane of the rolling direction and normal direction (RD-ND) was chosen for analysis. Samples for light microscopy (LM) and scanning electron microscopy (SEM) were prepared by mechanically polishing to 0.05 μm SiO_2 and etching in 2% Nital to reveal the lath martensitic microstructure.

The degree of microstructural refinement was assessed by measuring the PAG width and block size in the ausformed samples using the mean line intercept method. Concentric back scattered (CBS) detection mode was used in the SEM to distinguish orientation differences to help identify boundaries for block measurements.

Samples for Vickers hardness and tensile testing were cut from the ausformed coupons and plates in the longitudinal RD. Vickers hardness samples were ground to 1200 grit and hardness measurements for all samples were taken directly in center along the elongated microstructure in the RD on the RD-ND plane. The gauge length and width of the tested tensile samples were 3 mm and 1 mm respectively and tensile tests were conducted on a Test Resources 300 series testing machine with an initial strain rate of 0.005 s^{-1}.

2.3 Results

Single pass ausforming with varying rolling reductions and deformation temperatures was performed to develop the processing-microstructure-properties relationships of severely ausformed M54 steel and compare the effectiveness of ausforming to the conventional QT treatment.

2.3.1 Prior austenite grains (PAG)

Single pass ausforming resulted in elongated PAGs in the RD at all rolling reductions and deformation temperatures which indicates microstructural refinement (Fig. 2.5(a)-(c)). The PAG boundaries were clearly revealed under LM in all ausformed samples after mechanical polishing and etching but were not as obvious in the non-ausformed samples. From previous studies, the PAG size has been shown to be an important factor of martensite refinement, with smaller PAG sizes resulting in finer martensite blocks and packets [5, 11, 16].

a.

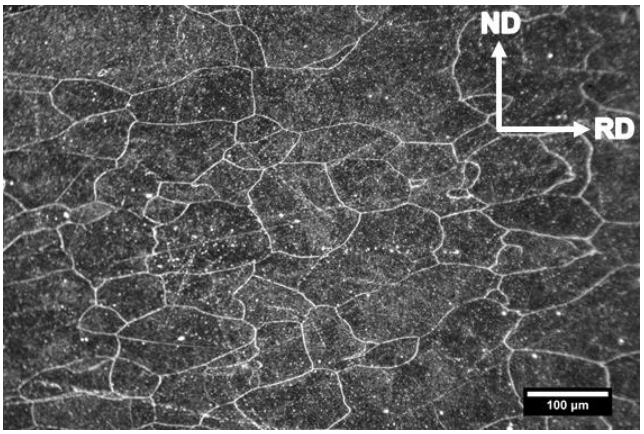

b.

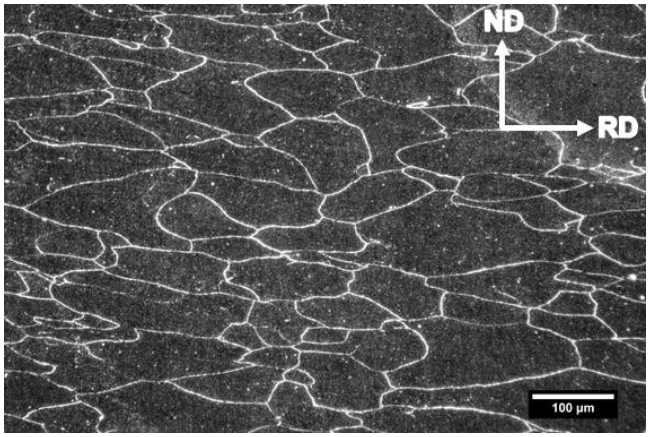

c.

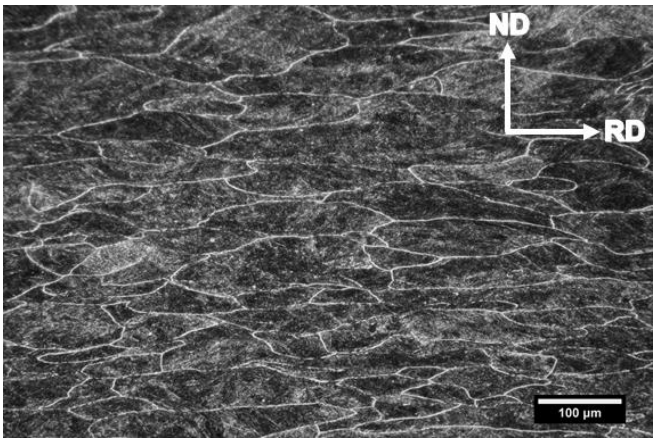

Fig. 2.5 Elongated (pancaked) PAGs in the RD on the RD-ND plane after (a) 30% reduction, (b) 45% reduction and (c) 60% reduction.

For the M54 steel samples, with the same rolling reductions, the ausformed PAG widths remained consistent at ~60, ~50 and ~40 μm after 30, 45, 60% ausforming at 550, 650 and 750°C (Fig. 2.6). The average PAG width of the ausformed full-scale plate was 33.4 ± 16.3 μm.

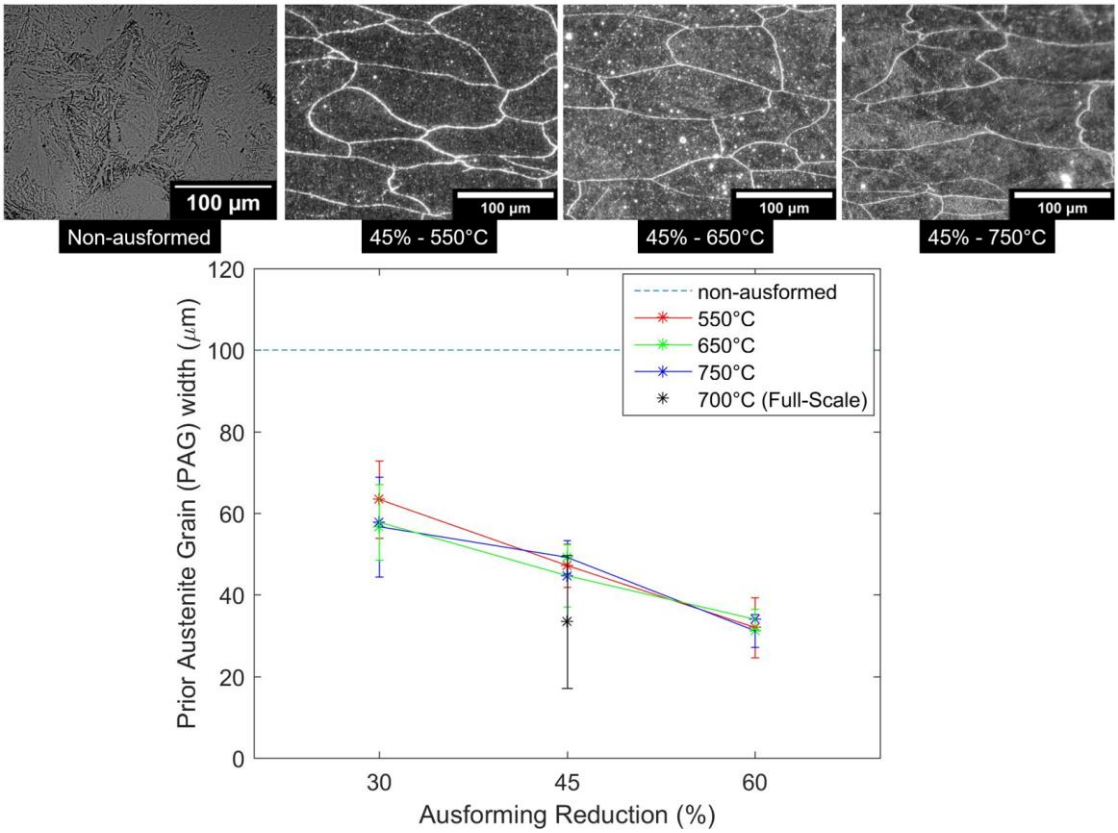

Fig. 2.6 Micrographs of (a) the non-ausformed sample and (b-d) pilot-scale coupons after 45% ausforming at 550, 650 and 750°C. (e) Average PAG width for non-ausformed and ausformed samples.

2.3.2 Lamellar Block Structures

Ultrafine lamellar block structures composed of blocks, sub-blocks and laths were also visible in the ausformed steel under SEM. Using the concentric backscattered (CBS) detector allowed contrasting high angle block boundaries to be identified and measured. The lamellar block structures became increasingly more refined with higher rolling reductions (Fig. 2.7(a)-(d)).

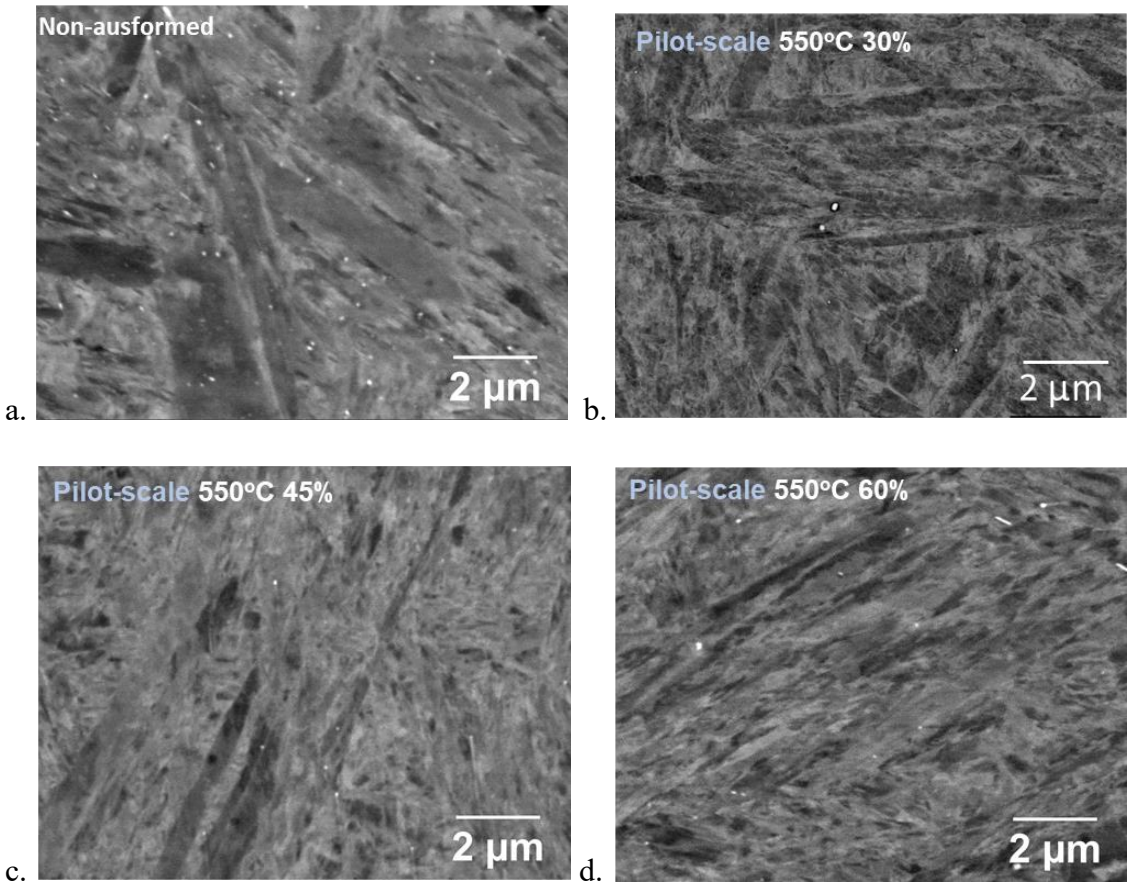

Fig. 2.7 SEM images of lamellar block structures with varying ausforming reductions: (a) non-ausformed, (b) 30% ausformed at 550°C, (c) 45% ausformed at 550°C and (d) 60% ausformed at 550°C.

The martensite structure of non-ausformed and ausformed M54 steel is composed of ultrafine block structures containing nanoscale substructures like sub-blocks and laths that could not be clearly defined with CBS detection in SEM (Fig. 2.7(a)-(d)). There were no significant differences in microstructure between the pilot-scale coupons that were 45% ausformed at 550, 650 and 750°C (Fig. 2.8(a)-(h)), however, the lamellar block structures in the full-scale plates appeared coarser than the pilot-scale coupons.

After 30, 45 and 60% ausforming at 550°C, the block width decreased from 1.10 μm to 0.653 μm, 0.471 μm and 0.240 μm.

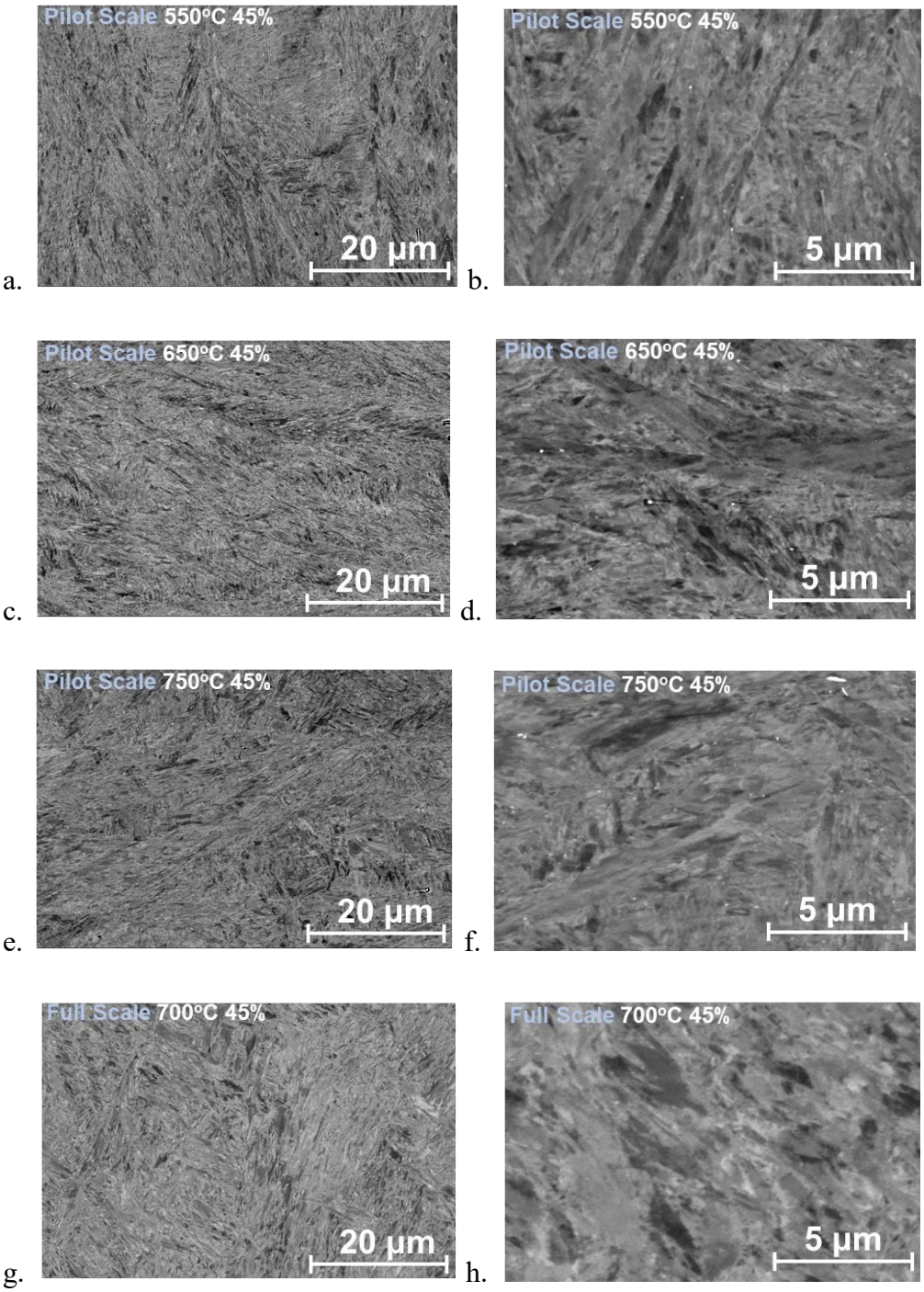

Fig. 2.8 SEM images of ausformed M54 after 45% reduction after pilot-scale ausforming at (a, b) 550°C, (c, d) 650°C, (e, f) 750°C and full-scale ausforming at (g, h) 700°C.

There was not a significant difference between the PAG and lamellar block widths after ausforming at different deformation temperatures with the same rolling reduction.

Fig. 2.9(a) shows the degree of block refinement after 30%, 45% and 60% ausforming at 550°C where block width is reduced from 1.10 µm (non-ausformed) to 0.653, 0.471 and 0.240 µm, respectively. After 45% pilot-scale ausforming with the pilot-scale samples at 550, 650 and 750°C, the resulting block widths were 0.471, 0.533 and 0.575 µm, respectively (Fig. 2.9(b)).

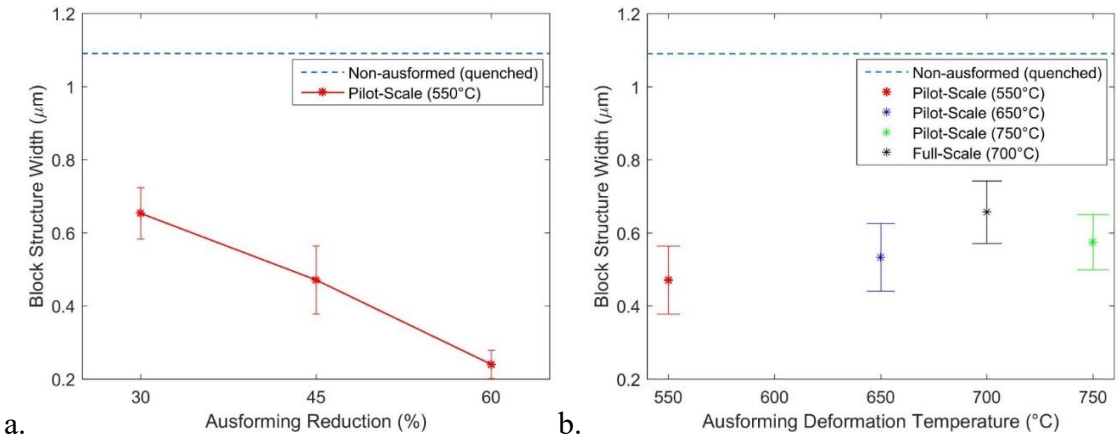

a. b.

Fig. 2.9 Average block structure widths of the non-ausformed sample and the ausformed samples after (a) 30% , 45% and 60% reduction and (b) 45% reduction at 550, 650, 700 (full-scale) and 750°C.

Of all the 45% ausformed samples, the microstructure of the full-scale plates appeared the most coarsened and had the largest block width of 0.657 µm. During full-scale ausforming, the plates were sent into the rollers at 700°C, however, since the rollers did not have heating capabilities, the plates quenched on the rollers during single pass rolling and the adiabatic heating spike due to the high rolling speed and reduction resulted in the plates being ausformed between 500°C - 700°C.

Further comparisons between the smaller substructures (sub-blocks, laths, dislocations) within the blocks were not performed. These required more advanced analysis techniques like transmission electron microscopy (TEM) to image and further study the nanoscale substructure features in the ausformed samples.

2.3.3 Vickers Hardness

Fig. 2.10 shows the variation in average hardness as a function of rolling reduction and deformation temperature. The hardness levels achieved after single pass ausforming were all significantly higher than the conventional QT hardness (606 HV) and increase with higher rolling reduction. The ausformed hardness levels were very similar after 30, 45 and 60% reduction at 550°C and 650°C, but the ausformed hardness after 45% and 60% reduction at 750°C were slightly lower than those ausformed at 550°C and 650°C with the same reductions. The ausformed hardness of the full-scale plates after 45% reduction between 500°C - 700°C was noticeably lower than the pilot-scale samples (~650 HV) but still greatly surpassed the QT hardness.

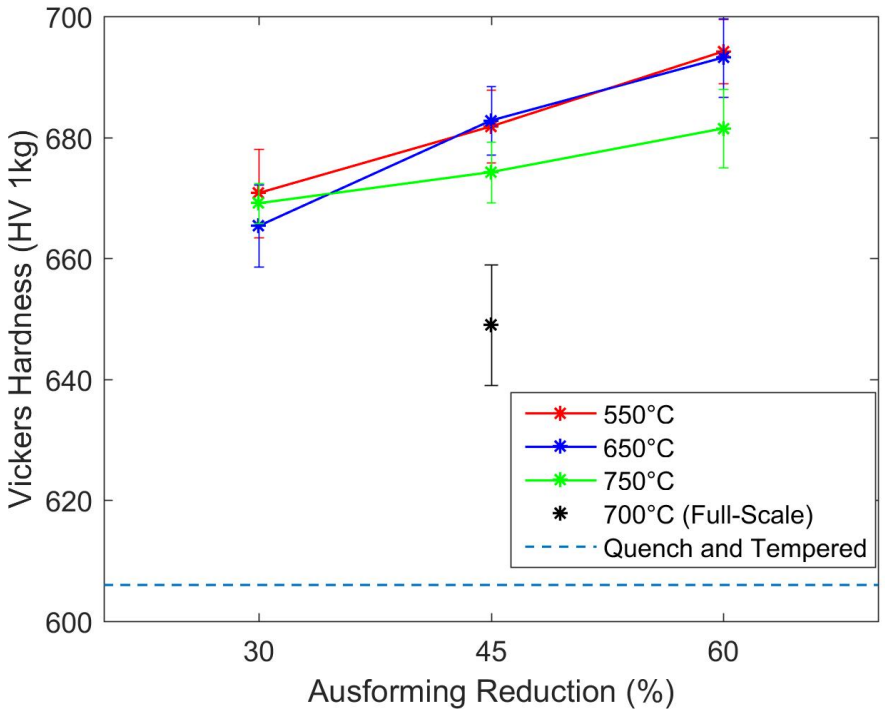

Fig. 2.10 Effect of ausforming reduction and deformation temperature on the hardness. The conventional QT hardness of M54 steel is shown as a reference (606 HV ≈ 54 HRC).

2.3.4 Tensile Testing

Tensile samples in the RD were cut from the pilot-scale coupon that was 45% ausformed at 550°C to compare with the 45% ausformed full-scale plates. The results were compared with the as-received (normalized) condition to show the outstanding increase in tensile strength while retaining good ductility (Fig. 2.11). The yield strength of the pilot-scale and full-scale ausformed sample increased from 1365 MPa to 1830 MPa and 1747 MPa, and the ultimate tensile strength increased from 1569 MPa to 2257 MPa and 2291 MPa while still retaining 14.4% and 13.4% elongation, respectively. The ausformed results also greatly exceeded the yield and ultimate tensile strength of the conventional QT condition (1730MPa and 2020 MPa).

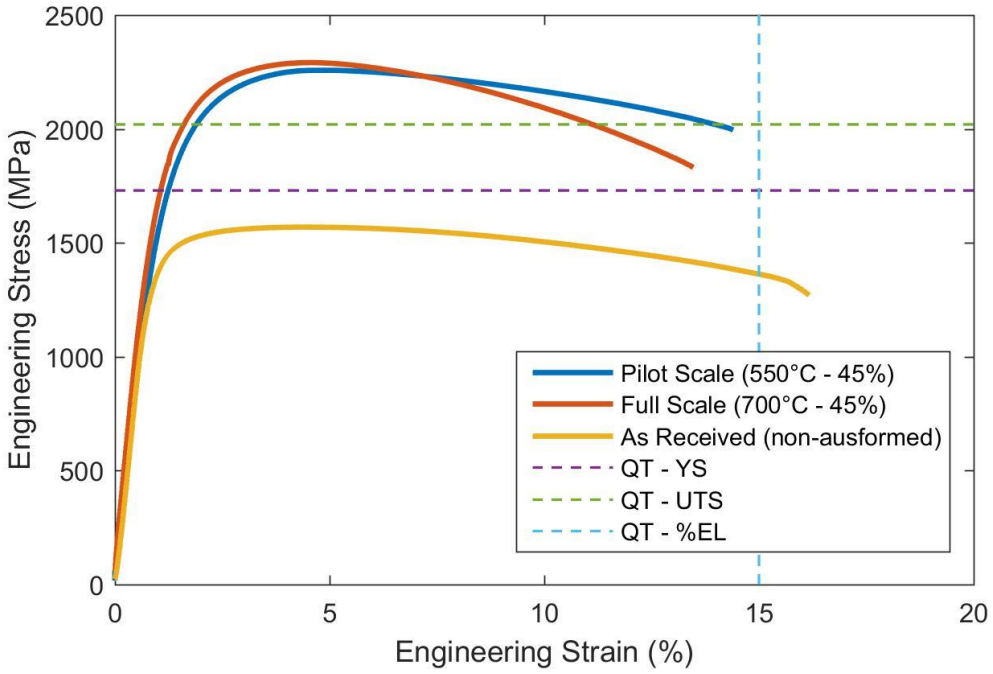

Fig. 2.11 Engineering stress-strain curves of ausformed and non-ausformed specimens.

2.4 Discussion

2.4.1 Rationale for Ausforming

During ausforming, strengthening is caused by a high density of dislocations and stored strain energy that can accumulate within the austenite when deformation occurs at lower temperature. The accumulation of defects and stored energy have been shown to effectively refine the hierarchical constituents of lath martensite [2, 3, 4, 17, 18]. Multi-pass rolling and/or high deformation temperature is typically needed to achieve high ausforming reductions due to the high flow stress of austenite. Therefore, less results are available regarding to single pass ausforming with high rolling reductions at lower temperature in recent SH-HA steels

Compared with multi-pass approach, however, single pass rolling at lower temperatures is still of great research interest because it can potentially further increase the dislocation density and stored strain energy in SH-HA steels [19]. As a result, less total rolling reduction may be required to achieve optimal microstructural refinement and mechanical properties. Meanwhile, M54 is a novel ultra-high strength steel recently designed, the effect of ausforming on M54 is yet to be revealed and the optimum ausforming parameters for M54 needs to be explored. SH-HA steels are currently being designed for a conventional QT process. With ausforming, future compositions can be optimized to take advantage of thermomechanical strengthening mechanisms instead of relying on expensive alloying additions and tempering to achieve ultra-high strength and good toughness through M_2C carbide precipitation. Ausforming can also be potentially used to enhance the secondary

hardening process when combined with tempering since dislocations are favorable sites for M_2C carbide nucleation.

Processing-Microstructure-Properties Relationships

Single pass ausforming of pilot-scale coupons with 30, 45 and 60% rolling reductions was performed at 550, 650 and 750°C to develop the processing-microstructure-properties relationships through microstructural analysis and mechanical testing. Increased dislocation density and stored strain energy were evidenced by degree of microstructural refinement (PAG and lamellar block width) and increased hardness. Additionally, single pass ausforming of full-scale plates with 45% rolling reduction at 700°C was performed to test scalability by comparing with the pilot-scale ausforming results.

Significant microstructural refinement and improved mechanical properties were observed in all pilot-scale coupons and full-scale plates after ausforming which agrees with prior studies which report that large strain deformation increases dislocation density and the amount of high angle boundaries which act as barriers to dislocation motion [4, 10]. The degree of refinement and hardness improvement was dependent on the rolling reduction and deformation temperature. Samples with the highest hardness levels after 60% ausforming also exhibited the most refined PAGs and lamellar block structures under LM and SEM.

The PAG and block structure widths were good indications of the degree of strengthening which agrees with prior studies that have verified the PAGs, packets and blocks as effective grain sizes for the Hall-Petch grain refinement relation observed in martensitic steels [6, 11, 20, 21, 22]. In the ausformed M54 steel, the high angle boundaries between packets

and blocks resulted in preferential etching making them visible in LM under certain conditions, however, the boundaries could not be confidently distinguished without knowing their exact crystallographic orientations. CBS detection provided orientation contrast in SEM to image and measure high angle lamellar block structures containing visible sub-block and lath structures, but it could not fully resolve the nanoscale laths.

Ausforming parameters are known to greatly affect the formation of the hierarchical packet/block/lath structure during martensitic transformation [5, 12, 23, 24, 25, 26]. The amount of rolling reduction affected the ausformed PAG width more strongly than the deformation temperature as evidenced by the similar PAG widths after ausforming at 550°C – 750°C. This highlights the processability of M54 steel for single pass ausforming to achieve uniform austenite grain refinement and work hardening within a wide temperature range (550°C - 750°C). However, at high deformation temperatures, adiabatic heating effects from high strain rates and extended processing times can cause microstructural changes like recovery, coarsening and recrystallization which result in less work hardening and coarser microstructures [23, 26, 27, 28, 29, 30].

In the present study as well, there was evidence of these changes during high temperature ausforming which indicated less refinement. The ausformed hardness measurements at 700°C and 750°C were slightly lower than their counterparts that were ausformed at 550°C and 650°C indicating less refinement which can be attributed to less work-hardening since the flow stress decreases with higher temperature [25]. Less stored strain energy and dislocations were able to accumulate at 750°C because the increased deformation

temperature and adiabatic heating effect both reduced the flow stress and accelerated the recovery and recrystallization processes [19, 29].

Similar behavior occurred in the full-scale plates after 45% rolling reduction at 700°C, which can be explained by the same rationale. However, the rolling mill used for the full-scale ausforming did not have heated rollers which caused the plates to quench on the rollers while ausforming. This roller-quenching effect counterbalanced the adiabatic heating effect during single pass, high reduction rolling which resulted in the plates being ausformed between 500°C -700°C. The reduced hardness in the full-scale plates compared to the pilot-scale coupons after 45% ausforming is likely due to the increased processing time and reduced control over sample temperature which resulted in a more coarsened microstructure.

Despite the differences in microstructure and hardness, the pilot-scale and full-scale samples after 45% ausforming both demonstrated enhanced mechanical properties during tensile testing. This may be because the rolling speed required for full-scale, single pass ausforming was 87.5 times faster than the pilot-scale and the flow stress increased with higher strain rate. Several studies have reported that higher strain rates generate more dislocations [12, 25]. Adiabatic heating effects are also amplified with higher strain rates, but this temperature spike was counterbalanced by the roll-quenching effect. These competing effects during full-scale ausforming may have resulted in the optimal combination of microstructural refinement, stored strain and dislocation density which agrees with recent studies by Lu and Ji concluding that deformation temperature and strain rate play similar roles on the dislocation density [25, 31]. Pilot-scale and full-scale

ausforming trials effectively refined the PAG and block structure widths, however, the packet refinement was not able to be quantified without more advanced analysis. Further investigation into the level of packet refinement after pilot-scale and full-scale ausforming may provide more insight into the enhanced mechanical behavior since prior studies by Wang showed the martensite packet size as the effective microstructural unit for cleavage fracture since high angle packet boundaries can strongly hinder fracture propagation [11].

2.5 Conclusion

In summary, the processing-microstructure-properties relationships of single pass ausforming with high rolling reduction (30/45/60%) at lower temperatures (550/650/750°C) was investigated in detail using a combination of LM, SEM and mechanical testing. Processability and scalability of single pass ausforming with M54 steel was verified by comparing the degree of microstructural refinement and strengthening in pilot-scale and full-scale samples after 45% rolling reduction. All single pass ausforming conditions produced a significantly more refined microstructure due to a higher density of dislocations and stored strain energy that accumulated at lower temperatures, leading to increased hardness and strength while retaining good ductility. Higher rolling reductions produced more refined PAGs and lamellar block structures as well as higher hardness levels. After 30, 45 and 60% ausforming at 550°C, the PAG size decreased from ~100 μm to ~60, ~50 and ~40 μm, block size decreased from 1.10 μm to 0.65, 0.47 and 0.24 μm and the hardness increased from 380 HV to ~670, ~680 and ~690 HV. These trends were consistent while ausforming at 650°C and 750°C as well, although at 750°C, the degree of

strengthening was slightly less due to the lowered flow stress and amount of work-hardening.

The ausformed full-scale samples achieved comparable PAG and block refinement and the pilot-scale samples and tensile tests showed that full-scale ausforming achieved similar tensile strengths as well which greatly surpassed the QT condition. The yield strength of the pilot-scale and full-scale ausformed sample increased from 1365 MPa to 1830 MPa and 1747 MPa, and the ultimate tensile strength increased from 1569 MPa to 2257 MPa and 2291 MPa while still retaining 14.4% and 13.4% elongation, respectively. Pilot-scale and full-scale results demonstrate SH-HA steels like M54 steel as promising candidates for future studies to develop and optimize alloys specifically for single pass ausforming at intermediate temperatures.

References

[1] T. V. Rajan, C. P. Sharma, and A. Sharma, Heat Treatment: Principles and Techniques. PHI Learning Pvt. Ltd., 2011.

[2] N. Tsuji and T. Maki, "Enhanced structural refinement by combining phase transformation and plastic deformation in steels," Scr. Mater., vol. 60, no. 12, pp. 1044–1049, Jun. 2009.

[3] E. I. Galindo-Nava and P. E. J. Rivera-Díaz-del-Castillo, "Understanding the factors controlling the hardness in martensitic steels," Scr. Mater., vol. 110, pp. 96–100, Jan. 2016.

[4] E. I. Galindo-Nava and P. E. J. Rivera-Díaz-del-Castillo, "A model for the microstructure behaviour and strength evolution in lath martensite," Acta Mater., vol. 98, pp. 81–93, Oct. 2015.

[5] Z. Li, X. Sun, Z. Yang, and Q. Yong, "Grain Refinement and Toughening of Low Carbon Low Alloy Martensitic Steel with Yield Strength 900 MPa Grade by Ausforming," in HSLA Steels 2015, Microalloying 2015 & Offshore Engineering Steels 2015, 2016, pp. 195–201.

[6] G. Krauss, "Martensite in steel: strength and structure," Materials Science and Engineering: A, vol. 273–275, pp. 40–57, Dec. 1999.

[7] S. Morito, H. Yoshida, T. Maki, and X. Huang, "Effect of block size on the strength of lath martensite in low carbon steels," Materials Science and Engineering: A, vol. 438–440, pp. 237–240, Nov. 2006.

[8] S. C. Kennett, G. Krauss, and K. O. Findley, "Prior austenite grain size and tempering effects on the dislocation density of low-C Nb–Ti microalloyed lath martensite," Scr. Mater., vol. 107, pp. 123–126, Oct. 2015.

[9] T. Karthikeyan, V. Thomas Paul, S. Saroja, A. Moitra, G. Sasikala, and M. Vijayalakshmi, "Grain refinement to improve impact toughness in 9Cr–1Mo steel through a double austenitization treatment," J. Nucl. Mater., vol. 419, no. 1, pp. 256–262, Dec. 2011.

[10] A. Belyakov, K. Tsuzaki, H. Miura, and T. Sakai, "Effect of initial microstructures on grain refinement in a stainless steel by large strain deformation," Acta Mater., vol. 51, no. 3, pp. 847–861, Feb. 2003.

[11] C. Wang, M. Wang, J. Shi, W. Hui, and H. Dong, "Effect of microstructural refinement on the toughness of low carbon martensitic steel," Scr. Mater., vol. 58, no. 6, pp. 492–495, Mar. 2008.

[12] M. Naderi, A. Saeed-Akbari, and W. Bleck, “The effects of non-isothermal deformation on martensitic transformation in 22MnB5 steel,” Materials Science and Engineering: A, vol. 487, no. 1, pp. 445–455, Jul. 2008.

[13] S. Tomoharu, T. Atsushi, T. Hidenori, and K. Yu-ich, “The Effects of Ausforming on Variant Selection of Martensite in Cr-Mo Steel,” 溶接学会論文集, vol. 31, no. 4, p. 178s–182s, 2013.

[14] S. Morito, I. Kishida, and T. Maki, “Microstructure of ausformed lath martensite in 18% Ni maraging steel,” in Journal de Physique IV (Proceedings), 2003, vol. 112, pp. 453–456.

[15] K. K. Sankaran and R. S. Mishra, Metallurgy and Design of Alloys with Hierarchical Microstructures. Elsevier, 2017.

[16] S. C. Kennett, G. Krauss, and K. O. Findley, “Prior austenite grain size and tempering effects on the dislocation density of low-C Nb–Ti microalloyed lath martensite,” Scr. Mater., vol. 107, pp. 123–126, Oct. 2015.

[17] S. Loewy, B. Rheingans, and E. J. Mittemeijer, “Transformation-rate maxima during lath martensite formation: plastic vs. elastic shape strain accommodation,” Philos. Mag., vol. 96, no. 14, pp. 1420–1436, May 2016.

[18] C. C. Kinney, K. R. Pytlewski, A. G. Khachaturyan, and J. W. Morris, “The microstructure of lath martensite in quenched 9Ni steel,” Acta Mater., vol. 69, pp. 372–385, May 2014.

[19] H. Beladi, G. L. Kelly, and P. D. Hodgson, “Microstructural evolution of ultrafine grained structure in plain carbon steels through single pass rolling,” Materials Science and Technology: MST; London, vol. 20, no. 12, pp. 1538–1544, Dec. 2004.

[20] J. P. Hirth, “The influence of grain boundaries on mechanical properties,” Metallurgical Transactions, vol. 3, no. 12, pp. 3047–3067, Dec. 1972.

[21] J. John William Morris, “On the Ductile-Brittle Transition in Lath Martensitic Steel,” ISIJ Int., vol. 51, no. 10, pp. 1569–1575, 2011.

[22] J. John William Morris, “Comments on the Microstructure and Properties of Ultrafine Grained Steel,” ISIJ Int., vol. 48, no. 8, pp. 1063–1070, 2008.

[23] M. Naderi and W. Bleck, “Martensitic Transformation during Simultaneous High Temperature Forming and Cooling Experiments,” Steel Res. Int., vol. 78, no. 12, pp. 914–920, Dec. 2007.

[24] H.-P. Li, R. Jiang, L.-F. He, H. Yang, C. Wang, and C.-Z. Zhang, “Influence of Deformation Degree and Cooling Rate on Microstructure and Phase Transformation Temperature of B1500HS Steel,” Acta Metall. Sin. , vol. 31, no. 1, pp. 33–47, Jan. 2018.

[25] J. Lu, Y. Song, L. Hua, J. Liu, and Y. Shen, “Influence of thermal deformation conditions on the microstructure and mechanical properties of boron steel,” Materials Science and Engineering: A, vol. 701, pp. 328–337, Jul. 2017.

[26] K. S. Cho et al., “Influence of rolling temperature on the microstructure and mechanical properties of secondary hardening high Co–Ni steel bearing 0.28wt% C,” Materials Science and Engineering: A, vol. 527, no. 27, pp. 7286–7293, Oct. 2010.

[27] Z. Zhu, W. Yuan, P. Zhang, and R. Zhang, “The Influence of High-Temperature Deformation and Heat Treatment on Microstructure of AF1410 Ultra-High Strength Steel,” Steel Res. Int., vol. 88, no. 12, p. 1700135, Dec. 2017.

[28] T. Sakai, A. Belyakov, R. Kaibyshev, H. Miura, and J. J. Jonas, “Dynamic and post-dynamic recrystallization under hot, cold and severe plastic deformation conditions,” Prog. Mater Sci., vol. 60, pp. 130–207, Mar. 2014.

[29] H. Mirzadeh and A. Najafizadeh, “Prediction of the critical conditions for initiation of dynamic recrystallization,” Mater. Des., vol. 31, no. 3, pp. 1174–1179, Mar. 2010.

[30] P. F. Giroux, F. Dalle, M. Sauzay, J. Malaplate, B. Fournier, and A. F. Gourgues-Lorenzon, “Mechanical and microstructural stability of P92 steel under uniaxial tension at high temperature,” Materials Science and Engineering: A, vol. 527, no. 16, pp. 3984–3993, Jun. 2010.

[31] G. Ji, F. Li, Q. Li, H. Li, and Z. Li, “Research on the dynamic recrystallization kinetics of Aermet100 steel,” Materials Science and Engineering: A, vol. 527, no. 9, pp. 2350–2355, Apr. 2010.

Chapter 3. Isothermal Tempering of Ferrium® M54® Steel after Single Pass Ausforming

Abstract

In the previous work, single pass ausforming of Ferrium® M54® was demonstrated to be an effective method to highly refine the hierarchical martensitic microstructure and achieve ultra-high strength while retaining good ductility without a need for a tempering treatment. In the present study, a processing route involving single pass ausforming and tempering was investigated to reveal the relationships between processing, microstructure and mechanical properties. Isothermal tempering studies were conducted between 350°C and 516°C after single pass ausforming and tensile tests were performed on fully processed material to evaluate the mechanical properties. Refinement of the tempered martensitic microstructure was assessed via scanning electron microscopy and hardness testing.

The combination of single pass ausforming and tempering has proven to be an effective way to highly-refine the martensitic microstructure and further enhance the mechanical properties of M54 steel via nanoprecipitate strengthening. After 45% single pass ausforming at 600°C and tempering at 425°C for 10 hours, the combination of yield strength, ultimate tensile strength and elongation were 1750 MPa, 2220 MPa and 17.3% which surpasses both the QT and as-ausformed (AF) conditions from the prior study.

3.1 Introduction

In recent years, nanoscale precipitation strengthening in lath martensitic steels has been receiving increasing interest and attention due to dramatic strength increases that have been achieved with almost no loss of ductility [1, 2, 3, 4]. This strengthening is due to the pinning of dislocations by finely dispersed nanoprecipitates that form during tempering. The precipitate type, size and number density are known to be critical factors that affect the degree of strengthening and toughening. However, this processing route can be expensive since some of these precipitate types can require high alloy additions and tempering treatments lasting up to 100 hours (h) to form the optimum size and number density that maximizes strength and toughness [5]. Studies have shown that dislocations are energetically favorable sites for precipitate nucleation during tempering and that by increasing the dislocation density and stored strain energy, the precipitation strengthening response can be improved and less alloy additions like Ni and Co may be required [6, 7, 8]. The thermomechanical controlled processing (TMCP) technique, ausforming, has been shown to be a promising method of maximizing dislocation density and stored strain energy in lath martensitic steels leading to an enhanced precipitation strengthening response [9, 10, 11].

In the prior study, single pass ausforming of a recently commercialized secondary hardening high-alloy (SH-HA) steel containing reduced Co content, Ferrium® M54®, has been shown to result in a work-hardened, refined lath martensite microstructure with strength and toughness levels exceeding the conventional QT condition. However, there are no studies on the tempering response in ausformed M54 steel. It may be possible to

further maximize the strength, hardness and ductility in SH-HA steels by combining ausforming and tempering to produce a work-hardened lath martensite microstructure strengthened by nanoscale M_2C carbides after tempering.

Nanoscale precipitation strengthening in lath martensitic steels is recognized as one of the most effective ways of improving strength without compromising ductility, however, the precipitation of finely dispersed nanoparticles can be expensive since it requires an extended tempering treatment at high temperature. This process is also referred to as precipitation hardening, age hardening (aging).

Fig. 3.1 shows the different stages of martensite tempering and what microstructural changes occur at each step. In stage I of tempering below 250°C, martensite softening occurs due to decomposition of supersaturated martensite into transition carbides and low carbon martensite [12]. Further softening occurs during the stages II and III due to cementite (Fe_3C) precipitation. However, in the fourth stage Fe_3C will begin to dissolve and either alloy carbides or intermetallic compounds will precipitate. Dislocations are also energetically favorable sites for M_2C carbide nucleation in SH-HA steels. Further details on the tempering stages and precipitation process have been investigated and described in literature [8, 13, 14, 15, 16, 17, 18, 19].

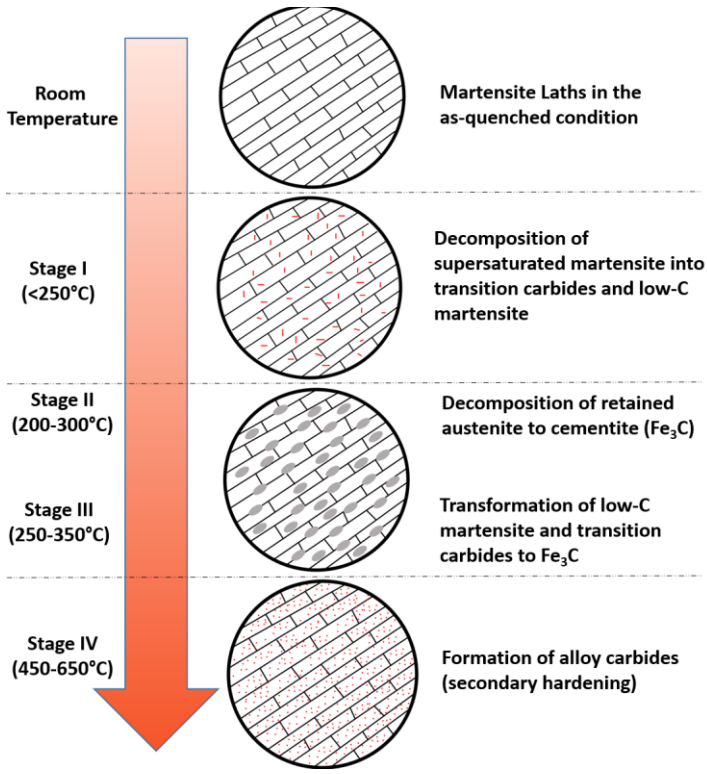

Fig. 3.1 The four stages of tempering for SH-HA steels and the microstructural changes that occur at each stage. Tempering information adapted from [12].

In a recent study by Won using differential scanning calorimetry (DSC), three exothermic events that correspond to various stages of tempering were observed during heating of severely ausformed SH-HA steels (80% total rolling reduction at 900°C) with varying Co content (5, 9 and 13 wt%) [20]. The addition of Co is known to raise the peak secondary hardening response in SH-HA steels by retarding dislocation recovery during tempering and providing additional chemical driving force for M_2C carbide nucleation [14, 21]. Fig. 3.2(a) shows the three exothermic events that took place in the temperature range of 50°C - 550°C. The first exothermic event is attributed to the precipitation of Fe_3C since it was observed between 150°C and 350°C. The second and third events which occurred between 350°C - 480°C and 480°C - 550°C, respectively, were attributed to the precipitation of M_2C carbides. Because M_2C carbides nucleate faster on Fe_3C than on dislocations, the second event was connected to the M_2C particles transformed from Fe_3C and the third event was connected to the well-known M_2C particles that nucleate on dislocations.

The results in Fig 3.2(b) and (c) show that an increase in Co content from 5 to 13 wt.% increased the hardness and tensile strength from 54.2 HRC to 57 HRC and 2028 MPa in the severely ausformed SH-HA steel after 5 h of tempering at 475°C. This improvement was attributed to the increased number density and dispersion of refined M_2C carbides.

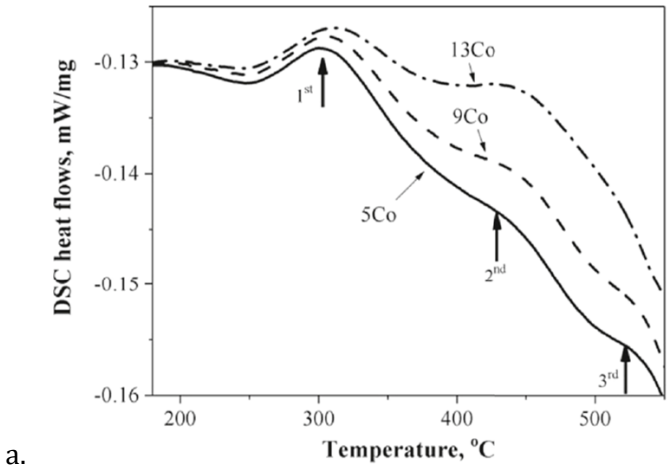

a.

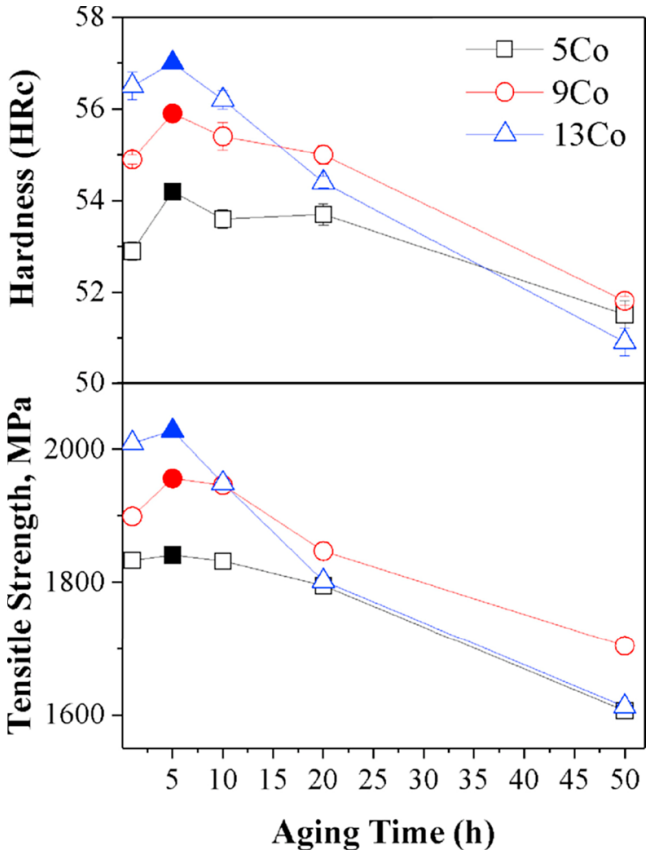

b.

Fig. 3.2 (a) DSC heat flow curves measured at a heating rate of 4 K/min. (b) Variation in Rockwell C hardness (HRC) and tensile strength (MPa) according to aging time for 80% ausformed SH-HA steels with 5, 9 and 13 wt. % Co isothermally aged at 475°C for 48 h [20].

In another study, Amirkamali also investigated the tempering behavior of a severely ausformed martensitic alloy, 17-4PH stainless steel [22]. After 70% ausforming at 400°C, the hardness increased from 32 HRC to 41.3 HRC due to significant lath refinement and increased dislocation density. Fig. 3.3(a) and (b) shows the precipitation hardening responses of non-ausformed and 70% ausformed 17-4PH steel while tempering at 300, 400, 500 and 600°C. The lowest tempering temperature, 300°C, displayed the weakest hardening response in both the ausformed and non-ausformed specimens. At 400°C, the responses were slow, but the hardness continued to increase throughout the entire 32 h treatment in both conditions. At 500°C, the 70% ausformed specimen had an accelerated response, reaching peak hardness in 1 h while the non-ausformed specimen took 2 h to reach peak hardness. At the highest tempering temperature, 600°C, the hardness increased minimally in both specimens after 1 h before drastically decreasing throughout the rest of the treatment due to coarsening and dislocation recovery. Fig. 3.3(c) shows the mechanical properties of the 70% ausformed specimens in the peak aged conditions. Although the peak aged condition was reached after 1 h at 500°C, the mechanical testing results showed that the peak aged condition after 32 h at 400°C exceeded both the yield and ultimate tensile strength as well as percent elongation. This was attributed to a finer distribution of precipitates that maintained coherency with the matrix in the peak aged condition at 400°C.

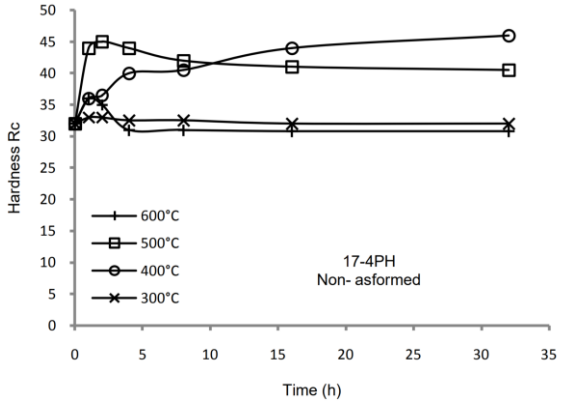

a.

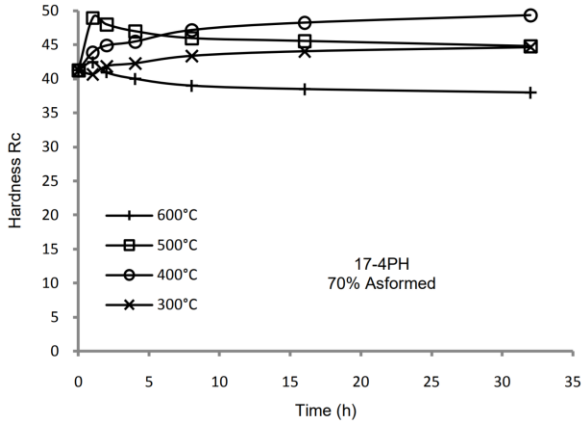

b.

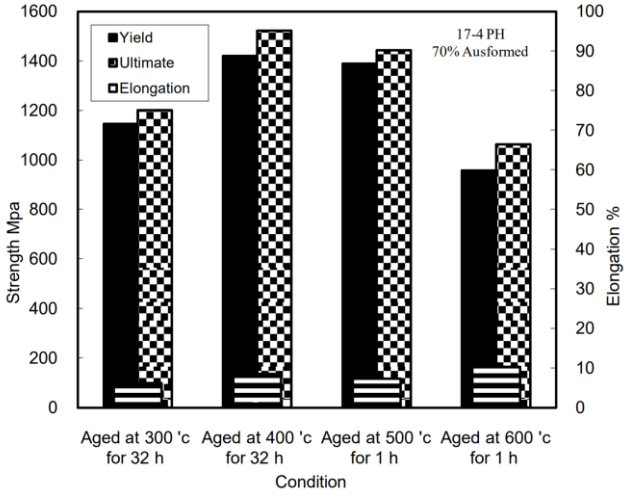

c.

Fig. 3.3 Variation of hardness of ausformed 17-4PH stainless steel samples in (a) non-ausformed and (b) 70% ausformed. (c) Plots of yield strength, ultimate tensile strength and elongation of 70% ausformed steel at peak aged conditions [22].

Due to the extremely high flow stress of SH-HA steels, multi-pass ausforming is usually required to achieve high rolling reductions, however, this can create issues with time and temperature control resulting in nonuniform ausforming, especially when reheating is required, and non-heated rolls are being used. In the present study, the influence of single pass ausforming on the secondary hardening behavior of M54 steel was investigated. M54 steel coupons were 45% ausformed via single pass warm rolling at 550°C and 600°C and subsequently tempered at 350, 425 and 516°C to analyze secondary hardening response and peak aged samples were selected for mechanical testing.

All ausformed samples had accelerated secondary hardening responses and showed higher resistance to softening in the early stages of tempering compared to the non-ausformed samples. The hardness increase associated with M_2C carbide precipitation begins after only 1 h in all the ausformed samples at all tempering temperatures, whereas softening in the non-ausformed samples lasted 2, 5 and 3 h at 516, 425 and 350°C before hardness began to increase. The ausformed sample that was peak aged at 425°C after 10 h had the best combination of mechanical properties in the peak aged conditions (1780 MPa yield strength (YS), 2220 MPa ultimate tensile strength (UTS) and 16.7% elongation (%EL)). In addition, the M54 coupons ausformed at 550°C and 600°C both showed very similar hardening responses at all tempering temperatures. Single pass ausforming has been shown to be an effective method to accelerate the secondary hardening process in M54 steel as well as improve resistance to softening and recovery during the early stages of tempering. The increased dislocation density and stored strain energy in ausformed M54 provided more energetically favorable nucleation sites and driving force for M_2C carbide

precipitation. Single pass ausforming combined with tempering at a lower temperature, 425°C, enhanced the effect of M_2C carbide strengthening in M54 steel which demonstrates the potential of single pass ausforming to improve the tempering response in SH-HA steels and further reduce the amount of expensive Co additions.

3.2 Materials and Methods

Raw M54 steel was provided by QuesTek Innovations in the normalized (annealed) form. The chemical composition of M54 steel is shown in Table 3.1 [12]. Non-ausformed M54 steel coupons were fabricated using a conventional QT heat treatment which is as follows. Austenitization (solution treatment) at 1060°C for 1 hour, oil quench to room temperature (RT), cryogenic treatment for 1 hour, air warm to RT, temper at 516°C for 10 hours and air cool to RT. It has been reported from previous studies on M54 steel that this QT schedule achieved the best combination of strength and ductility.

Table 3.1 Ferrium M54 chemical composition (nominal wt. %) [12].

Fe	C	Co	Cr	Ni	Mo	W	V
Bal.	0.3	7	1	10	2	1.3	0.1

The shape and dimensions of the M54 steel coupons for single pass warm rolling are shown in Fig. 3.4. The tapered coupons were cut using wire electrical discharge machining (EDM). The tapered coupons were austenitized at 1060°C for 1 hour, followed by single pass ausforming at either 550°C or 600°C with a rolling reduction of 45%. The ausformed M54 steel coupons were immediately oil quenched to room temperature and transferred to

a liquid nitrogen bath for 1 hour to achieve full lath martensitic transformation. After air warming to RT, Vickers hardness measurements (HV 1kg) were taken in the center of the coupons along the RD on the RD-ND plane.

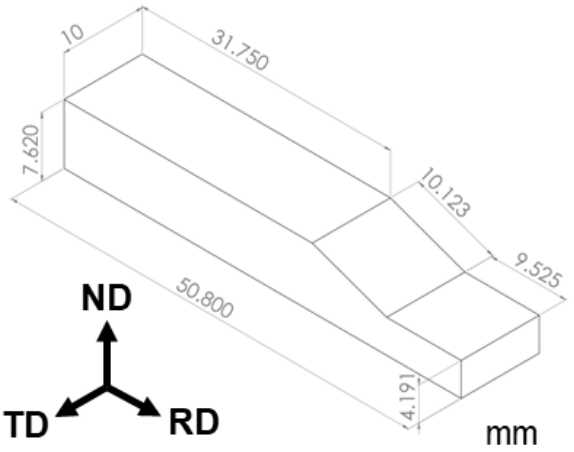

Fig. 3.4 Dimensions of M54 steel coupon tapered for 45% single pass rolling reduction (mm). Rolling, transverse and normal directions are denoted by RD, TD and ND.

Both ausformed and non-ausformed samples of M54 steel were sectioned into small blocks approximately 3 mm x 10 mm x 4 mm and subjected to the conventional high temperature tempering (HTT) treatment at 516°C for 10 hours to observe the secondary hardening responses. Intermediate temperature tempering (ITT) treatments at 425°C and 350°C for 48 hours were also conducted to compare the non-ausformed and ausformed secondary hardening responses at reduced tempering temperatures.

The HTT and ITT treatments for all ausformed and non-ausformed samples were performed in a Sentrotech box furnace. Vickers hardness (HV 1kg) measurements were taken after 1, 2, 3, 5, 7 and 10 hours in the center of the samples on the RD-ND plane containing the elongated work-hardened PAGs as depicted in Fig 3.5. The average of 15

indentations was taken for each condition to minimize error. For the ITT treatments, Vickers hardness was also measured after 16, 24 and 48 hours. Samples that showed the best results in hardness measurement were selected for microstructural analysis and tensile testing.

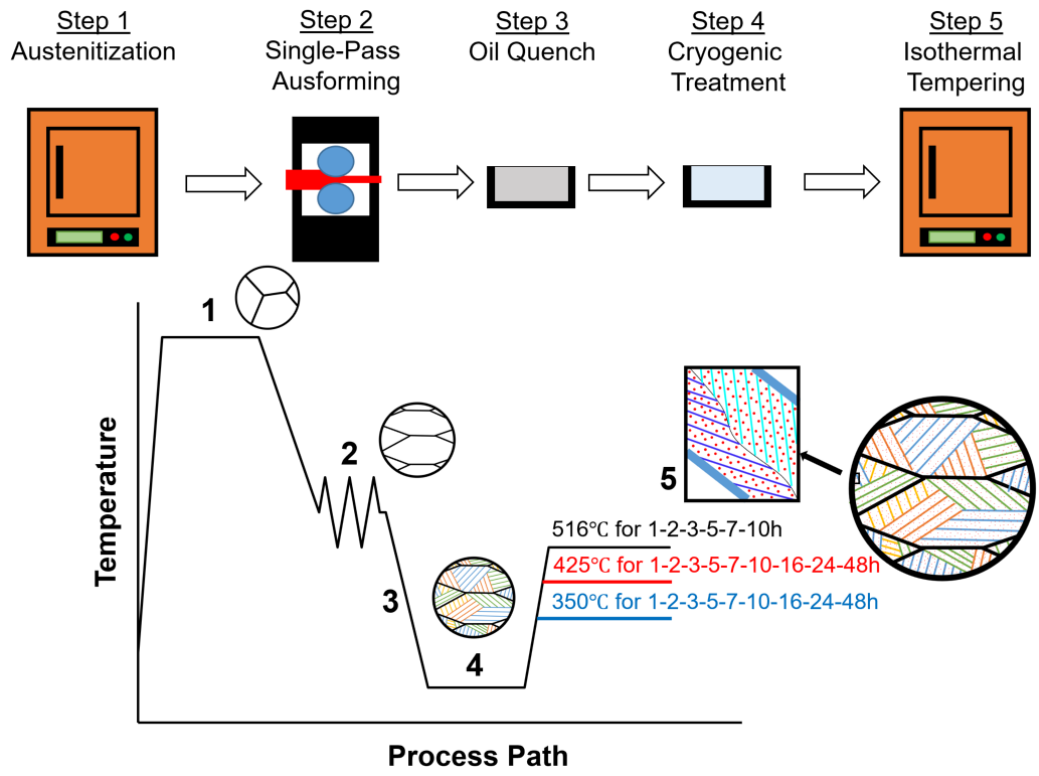

Fig. 3.5 Processing path for single pass ausforming followed by isothermal tempering.

Tensile testing samples were cut from the ausformed and tempered coupons on the RD-TD plane. The gauge length and width of the tested tensile samples were 3 mm and 1 mm respectively and tensile tests were conducted on a Test Resources 300 series testing machine with an initial strain rate of 0.005 s^{-1}.

3.3 Results

3.3.1 As-Quenched Vickers Hardness

Vickers hardness measurements were taken in the as-quenched (AQ) condition obtained after cryogenic treatment for both ausformed and non-ausformed samples. The results are shown in Table 3.2. The AQ hardness measurements of the samples ausformed at 550°C and 600°C were both extremely similar (~680 HV) and higher than the non-ausformed sample.

Table 3.2 As-quenched (AQ) hardness of ausformed and non-ausformed coupons prior to tempering

Processing condition	Hardness (HV 1kg)	Standard Deviation	Number of Measurements
Ausformed (45% at 550°C)	681	5.95	30
Ausformed (45% at 600C)	677	6.56	35
Non-ausformed	640	7.24	10

3.3.2 Aging Curves

The age hardening (aging) curves are shown in Fig. 3.6(a)-(c) and the peak aged hardness responses during tempering for each condition are summarized in Table 3.3. An average of 15 hardness indentations were measured for each condition. Regardless of the tempering temperature, the two ausforming conditions exhibited very similar age hardening behavior with similar peak hardness values, while the non-ausformed samples always showed lower hardness values throughout the tempering process.

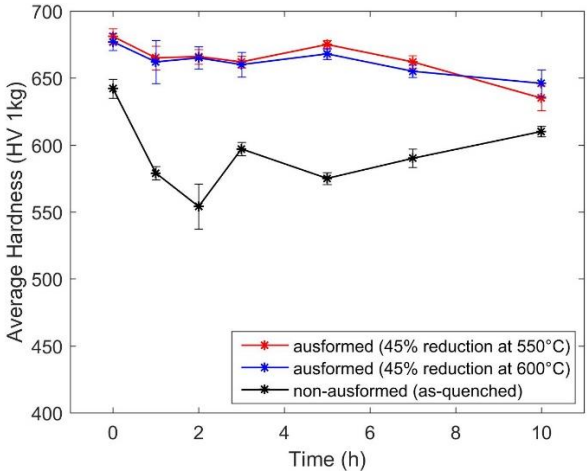

a.

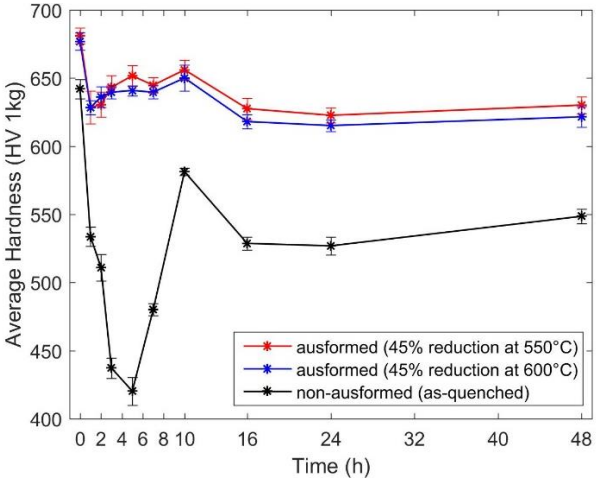

b.

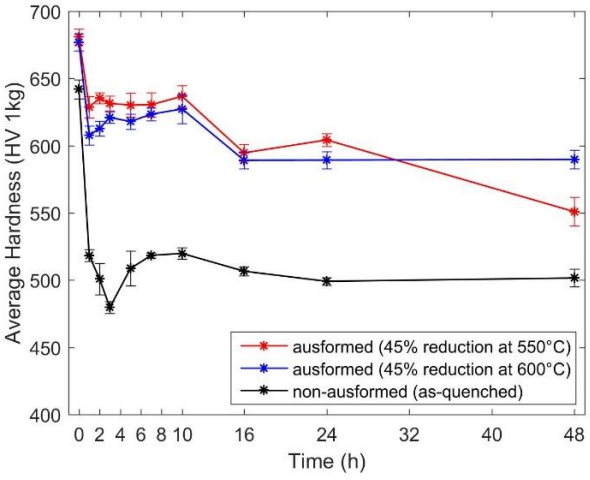

c.

Fig. 3.6 Variations in average hardness according to tempering time at (a) 516°C, (b) 425°C and (c) 350°C

At the 516°C tempering temperature, both of the ausformed samples reached their peak hardness of around 670 HV after only 5 hours while the non-ausformed sample required the regular 10 hours to reach it's peak hardness of 610 HV (~54 HRC). At 425°C and 350°C, all the samples reached their peak hardness conditions after 10 hours of tempering, but the peak hardness response decreased with reduced tempering temperatures for both ausformed and non-ausformed samples. The maximum hardness levels that were achieved in the ausformed samples at reduced tempering temperatures were ~650 HV at 425°C and ~630 HV at 350°C after 10 hours.

Table 3.3 Hardness measurements and isothermal tempering durations of the peak aged conditions during HTT and ITT

	516°C		425°C		350°C	
	Peak Aged Hardness (HV 1kg)	Isothermal Tempering Duration (h)	Peak Aged Hardness (HV 1kg)	Isothermal Tempering Duration (h)	Peak Aged Hardness (HV 1kg)	Isothermal Tempering Duration (h)
45% ausformed at 550°C	675±3.26	5	656±7.16	10	637±8.14	10
45% ausformed at 600°C	668±4.04	5	650±9.54	10	627±10.8	10
Non-ausformed	610±3.96	10	581±2.65	10	520±4.23	10

An initial hardness drop was observed in all aging curves but was more severe for the non-ausformed samples. During tempering at 516, 425 and 350°C, the initial drops of the non-ausformed samples were 90, 220 and 160 HV after 1, 5 and 3 h, respectively.

The hardness initially decreased in the ausformed samples as well, but the drops are lower in magnitude and the hardness begin to increase within the first hour, whereas drops in the non-ausformed samples lasted 2 - 5 h before hardness increased. At 516°C, softening only reduces the ausformed hardness by ~20HV, but at 425 and 350°C, resistance to softening decreased and the hardness reductions within the first hour increase to ~50HV and ~60HV, respectively.

3.3.3 Peak Aged Microstructure

Microstructural analysis via scanning electron microscopy (SEM) was performed on the peak aged samples as well but since the M_2C carbides are expected to be nano-sized, which is beyond the resolution of a typical SEM, there were no clear distinctions between the aged microstructures except that the ausformed samples possessed a more refined lath structure as shown in Fig. 3.7(a) and (b). High resolution transmission electron microscopy (HR-TEM) or atom probe tomography (APT) is required to do further analysis of size and number density of the M_2C carbides to compare the nanoscale differences between aged samples and analyze the interactions between dislocations and precipitates.

a.

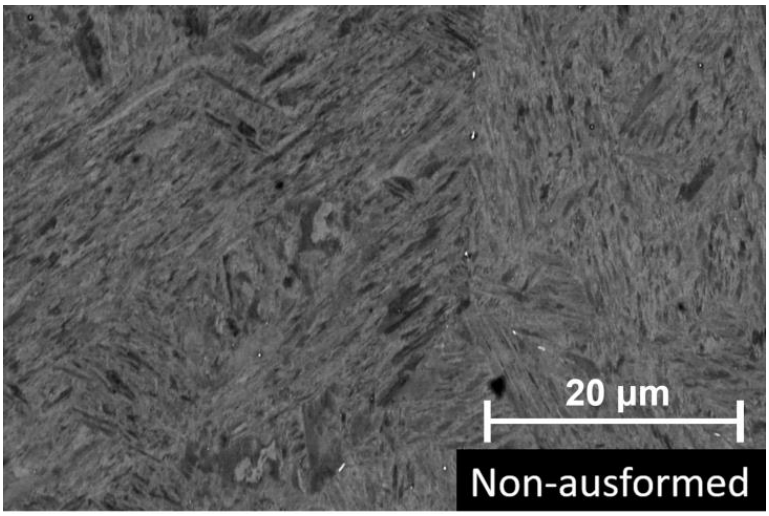

b.

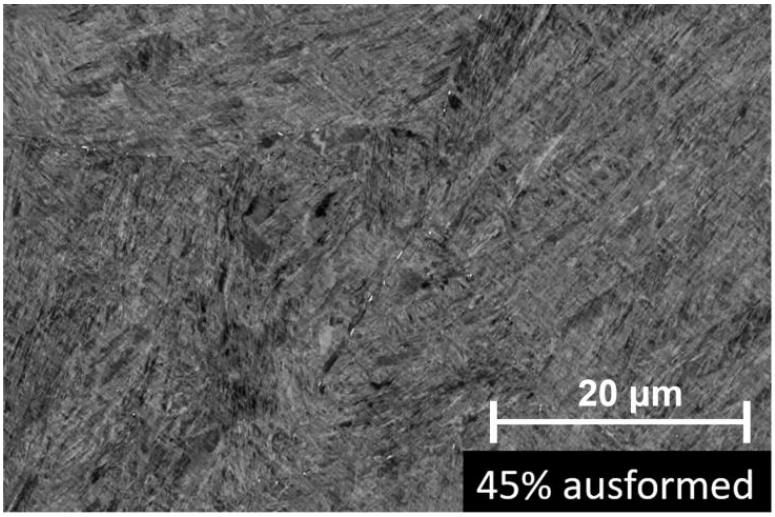

Fig. 3.7 SEM images of (a) non-ausformed and (b) 45% ausformed M54 steel in the peak aged condition at HTT (516°C).

3.3.4 Tensile Testing

Tensile test specimens were cut from the ausformed samples that were aged at 350 for 10 h, 425 for 10 h and 516°C for 5 h, corresponding to the peak hardness conditions, and tested to compare with the conventional QT condition which possesses 1730MPa YS, 2020 MPa ultimate tensile strength and 15% elongation. The samples that were tempered at 516°C

and 350°C had similar YS (1759 MPa and 1724 MPa) and UTS (2060 MPa and 2040 MPa) with the former having slightly better ductility (16.7% and 15.7% elongation), and the sample that was tempered at 425°C for 10 hours exhibited the best combination of YS, UTS and ductility (1750MPa, 2220 MPa and 17.3% elongation) (Fig. 3.8). The variations between the tested specimens with different conditions were not completely consistent with the hardness results (Fig 3.3). Possible reasons include heterogeneity of warm rolled specimens as well as different stress conditions between hardness indentation and uniaxial tension. However, the fully processed (ausforming and tempering) M54 specimens did exhibit excellent combinations of strength and ductility with ultimate tensile strengths over 2000 MPa and elongations about 15%.

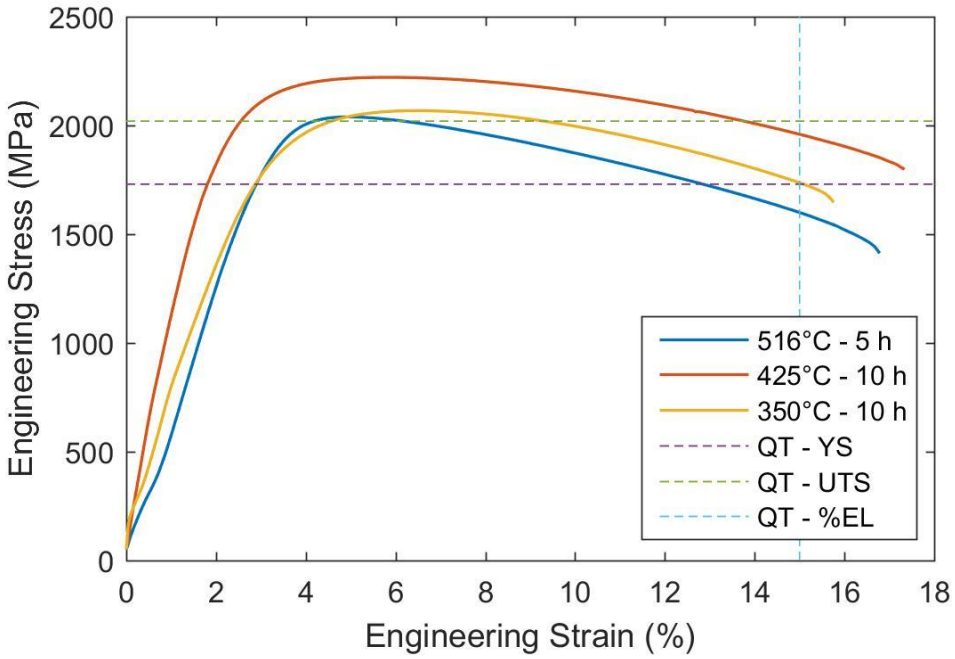

Fig. 3.8 Stress-strain curves of ausformed samples in the peak aged condition at HTT (516°C) and ITT (425 and 350°C)

3.4 Discussion

3.4.1 Rationale for Ausforming

In addition to the microstructure refinement effect discussed in the previous chapter, low temperature single pass ausforming also has the great potential to improve the current processing route of SH-HA steels by increasing the stored strain energy and dislocation density [23, 24, 25]. During the subsequent tempering, additional benefits on the mechanical properties could potentially be obtained through the process of martensite softening and carbide precipitation. The increased dislocation density and stored strain energy provides the optimal conditions for an enhanced secondary hardening response during tempering, which can improve the strength and ductility combination while reducing the necessary time to achieve the peak hardening condition. Expensive Co alloy additions may possibly be reduced as well because of the precipitation acceleration effect from ausforming. M54 steel coupons were ausformed via single pass warm rolling and subsequently tempered to produce work-hardened lath martensite microstructures strengthened by M_2C carbide precipitates. To investigate the effectiveness of single pass ausforming, tempering was performed at 516, 425 and 350°C. Hardness was measured at different tempering times as an indication of the secondary hardening behavior of severely ausformed M54 steel at reduced tempering temperatures. The microstructure was also characterized to investigate the possible relationships between hardness change and microstructure evolution during tempering. For comparison, non-ausformed M54 steel coupons were also subjected to the same tempering treatments as the ausformed coupons.

3.4.2 Effect of Ausforming on the Tempering Response

Two major differences were observed between the non-ausformed and ausformed samples at all three tempering temperatures. The ausformed samples had an accelerated secondary hardening response as well as higher resistance to martensite softening in the early stages of tempering. The accelerated response agrees with existing literature results since ausforming results in higher dislocation density and stored strain energy which provides more energetically favorable nucleation sites and driving force for M_2C carbide precipitation [26, 27]. However, resistance to softening and accelerated hardening behavior in the ausformed samples decreased with lowered tempering temperature. This behavior can be explained by previous works that report on the microstructural and property changes that occur in lath martensite during tempering at intermediate and high temperatures [19]. In the present study, tempering at 325 and 425°C is considered intermediate temperature tempering (ITT) and while 516°C is considered high temperature tempering (HTT).

In early stages of HTT it is well documented that the substitutional alloying elements strongly retard softening when they concentrate in cementite [19, 28]. The enriched cementite particles pin lath boundaries and contribute to the ability to resist initial rapid softening due to crystal coarsening. Conversely, during the early stages of ITT, those same alloying elements do not concentrate into cementite. These elements which stabilize cementite do not have sufficient diffusional mobility during early stages of ITT to form enriched particles. Therefore, these cementite particles, made only of iron and carbon, coarsen and softening resistance is diminished. This same behavior was also observed and

confirmed by APT in a recent study where 4340 steel was quenched and tempered at 325, 450 and 575°C for 2 h [28].

The martensite softening effect was far more drastic in the non-ausformed tempering curves compared to the ausformed curves, especially during ITT. This highlights the potential of ausforming as a technique to enhance softening resistance at lower tempering temperatures. Since dislocation density is a major contributor to hardness at any stage of tempering, the higher dislocation density and stored strain energy in the ausformed samples may be providing the additional driving force needed to speed up M_2C carbide precipitation and allow carbide forming elements to concentrate into cementite at early stages in ITT [6, 27].

3.4.3 Ausformed and Tempered Mechanical Properties

Although the highest ausformed peak hardness response was achieved in HTT (516°C for 5 h), the ausformed sample that underwent ITT (425°C for 10 h) resulted in a better combination of strength and ductility during tensile testing (Fig. 3.8). This is most likely due to microstructural changes that occur during tempering which are deeply affected by temperature like lath/precipitate coarsening and dislocation recovery. These changes are all accelerated at higher temperatures. A recent review by Kong provides an in-depth analysis on how size, number density and coherency of the M_2C carbides are significant factors that influence strengthening because of how each factor affects precipitate-dislocation interactions [5]. The effects of these changes were also seen in Amirkamali's results in Fig. 3.3 where HTT at 500°C for 1 h lead to coarsening of precipitates, while ITT at 400°C for 32 h led to a very uniform size and homogeneous dispersion of precipitates

[22]. Similarly, Cho also reported faster coarsening and loss of coherency at high tempering temperature in cementite-nucleated M_2C carbides [6, 27].

Therefore, in the present study, the gradual hardness increase seen in the ausformed sample during ITT at 425°C could indicate that the size of the precipitates was growing but has not yet coarsened and a finer, more uniform and coherent dispersion was achieved compared to HTT at 516°C. This agrees with other studies that have shown low temperature severe ausforming to be an effective method for refining M_2C carbides.

The YS and UTS of the peak aged samples at 516°C and 350°C were similar but with the former having slightly better ductility. This may also be attributed to the accelerated M_2C carbide precipitation, recovery of dislocations and lath/precipitate coarsening in HTT versus ITT.

Based on the earlier discussion of HTT, the cementite-nucleated M_2C carbides may have rapidly coarsened and lost coherency leading to reduced strength while the overall higher number density of nanoprecipitates due to the overall higher driving force for precipitation could be the reason why ductility was slightly better. Minimal strength and ductility improvement was seen in the ausformed sample that was tempered at 350°C for 10 h. There may not have been enough driving force at 350°C, even after single pass ausforming, for enriched cementite particles to form and pin lath boundaries and subsequently form the optimal size, number density and dispersion of M_2C carbides to resist softening and recovery mechanisms.

3.4.4 Additional Findings

It is also worth noting that only 45% rolling reduction in single pass ausforming was required to produce similar peak hardness and higher tensile strength in M54 steel (7 wt% Co) after tempering, that was achieved through 80% multi-pass rolling reduction in a SH-HA steel containing 13 wt% Co: 57 HRC (~694 HV) and 2028 MPa respectively (Fig. 3.2(b) and (c)) [20]. Since the early work in the 1960's on lath martensite tempering by Speich and Leslie, high Co additions have been observed to suppress dislocation recovery during tempering and increase both the dislocation density and chemical driving force for M_2C carbide precipitation [13, 15, 19]. The results of single pass ausforming at low temperature with M54 could potentially mean that Co additions could be further lowered with higher single pass rolling reductions or decreasing deformation temperature, both of which would increase dislocation density and stored strain energy.

It is also interesting to note that the samples ausformed at 550°C and 600°C had very similar secondary hardening responses throughout tempering (Fig. 3.6(a)-(c)) which indicates good processability of M54 steel since deformation temperature greatly influences the degree of microstructural refinement and dislocation density in ausformed steels.

3.4.5 Future Work

Overall, it has been concluded that the major parameters and mechanisms that influence strengthening during HTT and ITT are dislocation density, stored strain energy, resistance to martensite softening and lath/carbide coarsening, carbide number density/dispersion and dislocation-carbide interactions. However, many of these behaviors and changes occurring

at the dislocation/carbide scale were unable to be quantitatively investigated in the present study. Further analysis with sophisticated imaging techniques such as HR-TEM and APT is required to perform direct observations and measurements. Line profile analysis of x-ray diffraction (XRD) data can also be used to measure dislocation density and study stored strain using peak broadening. The effect of increased dislocation density and stored strain energy during tempering can be also be studied with DSC experiments. The heating parameters and results can be used to calculate the effective activation energy by the modified Kissinger method and how it is affected by the degree of ausforming [6, 27].

3.5 Conclusion

In summary, by developing the processing-microstructure-properties relationships of single pass, low temperature ausforming combined with ITT, future SH-HA steel compositions can potentially be optimized so that they do not rely on expensive alloying additions and HTT to obtain optimal dislocation density and carbide precipitation but instead utilize the benefits of ausforming. In the current study, the effect of single pass, 45% reduction ausforming at 600°C on the secondary hardening behavior was analyzed at HTT (516°C) and ITT (425°C and 350°C), the results of which can be summarized as follows:

Single pass ausforming increased resistance to softening during the early stages of tempering and accelerated the secondary hardening process. The difference in hardness reduction during softening between the non-ausformed and ausformed samples were 90 HV to 20 HV at 516°C, 220 HV to 50 HV at 425°C and 160 HV to 60 HV at 350°C. During ITT (425°C and 350°C), rapid softening occurred in the non-ausformed samples, perhaps

due to the lack of diffusional mobility at lower temperatures for enriched cementite to form, but for the ausformed samples, the increased dislocation density and stored strain energy seemed to provide the additional nucleation sites and driving force needed for the precipitation of M_2C carbides which counteract the softening effect. Additionally, these ausforming effects also caused the hardness of the ausformed samples to increase after only 1 h at all tempering temperatures, while the non-ausformed hardness did not increase until after 2, 5 and 3 h at 516, 425 and 350°C respectively.

Tempering of the ausformed M54 samples improved the combination of yield strength, ultimate tensile strength and percent elongation compared to the conventional QT form (YS: 1730MPa, UTUS: 2020 MPa and EL: 15%). After tempering for 5, 10 and 10 h at 516, 425 and 350°C, respectively, the yield strengths were 1759, 1750 and 1724 MPa, ultimate tensile strengths were 2040, 2220 and 2060 MPa and elongations were 16.7, 17.3 and 15.7%. These results were also attributed to the effects of increased dislocation density and stored strain energy after single pass, low temperature ausforming.

Table 3.4 compares the peak 45% ausformed and tempered (AT) condition with the 45% as-ausformed (AF) pilot-scale and full-scale conditions from the prior study.

Table 3.4 Peak conditions from both ausforming studies compared to the QT condition

	QT	Pilot-Scale (45% - 550°C)	Full-Scale (45% - 700°C)	Ausformed and Tempered (45% - 600°C, 425°C for 10 h)
YS (MPa)	1730	1830	1747	1750
UTS (MPa)	2020	2257	2291	2221
EL (%)	15	14.4	13.4	17.3

The combination of strength and ductility in the AT and AF conditions both surpassed the QT condition. The AT and AF both achieved similar tensile strengths, however, the AT achieved higher ductility levels due to the combination of microstructural refinement from ausforming which increases the amount of high angle grain boundaries nanoprecipitates and nanoprecipitate strengthening from tempering. Ausforming has proven to be a robust processing route for SH-HA steels and a potential way to improve future alloy and processing design strategies for ultra-high strength steel products

References

[1] S. Jiang *et al.*, "Ultrastrong steel via minimal lattice misfit and high-density nanoprecipitation," *Nature*, vol. 544, no. 7651, pp. 460–464, Apr. 2017.

[2] Z. B. Jiao, J. H. Luan, M. K. Miller, Y. W. Chung, and C. T. Liu, "Co-precipitation of nanoscale particles in steels with ultra-high strength for a new era," *Mater. Today*, vol. 20, no. 3, pp. 142–154, Apr. 2017.

[3] J. W. Morris Jr, "Maraging steels: Making steel strong and cheap," *Nat. Mater.*, vol. 16, no. 8, pp. 787–789, Jul. 2017.

[4] G. B. Olson, "Genomic materials design: The ferrous frontier," *Acta Mater.*, vol. 61, no. 3, pp. 771–781, Feb. 2013.

[5] H. J. Kong and C. T. Liu, "A Review on Nano-Scale Precipitation in Steels," *Technologies*, vol. 6, no. 1, p. 36, Mar. 2018.

[6] K. S. Cho *et al.*, "Influence of rolling temperature on the microstructure and mechanical properties of secondary hardening high Co–Ni steel bearing 0.28wt% C," *Materials Science and Engineering: A*, vol. 527, no. 27, pp. 7286–7293, Oct. 2010.

[7] A. Mondiere, V. Déneux, N. Binot, and D. Delagnes, "Controlling the MC and M2C carbide precipitation in Ferrium® M54® steel to achieve optimum ultimate tensile strength/fracture toughness balance," *Mater. Charact.*, vol. 140, pp. 103–112, Jun. 2018.

[8] G. R. Speich, D. S. Dabkowski, and L. F. Porter, "Strength and toughness of Fe-10ni alloys containing C, Cr, Mo, and Co," *Metallurgical Transactions*, vol. 4, no. 1, pp. 303–315, Jan. 1973.

[9] L. Lv, L. Fu, Y. Sun, and A. Shan, "An investigation on the microstructure and mechanical properties in an ultrafine lamellar martensitic steel processed by heavy warm rolling and tempering," *Materials Science and Engineering: A*, vol. 731, pp. 369–376, Jul. 2018.

[10] N. Tsuji and T. Maki, "Enhanced structural refinement by combining phase transformation and plastic deformation in steels," *Scr. Mater.*, vol. 60, no. 12, pp. 1044–1049, Jun. 2009.

[11] R. L. Klueh, N. Hashimoto, and P. J. Maziasz, "Development of new nano-particle-strengthened martensitic steels," *Scr. Mater.*, vol. 53, no. 3, pp. 275–280, Aug. 2005.

[12] K. K. Sankaran and R. S. Mishra, Metallurgy and Design of Alloys with Hierarchical Microstructures. Elsevier, 2017.

[13] G. R. Speich, “Tempering of low-carbon martensite,” *Trans Met Soc AIME*, vol. 245, no. 12, pp. 2553–2564, 1969.

[14] G. R. Speich, “Secondary Hardening Ultrahigh-Strength Steels,” *Innovations in Ultrahigh Strength Steel Technology*, pp. 89–112, 1990.

[15] G. R. Speich and W. C. Leslie, “Tempering of steel,” *Metallurgical Transactions*, vol. 3, no. 5, pp. 1043–1054, May 1972.

[16] Y. Ohmori and I. Tamura, “Epsilon carbide precipitation during tempering of plain carbon martensite,” *Metall. Trans. A*, vol. 23, no. 10, pp. 2737–2751, Oct. 1992.

[17] C. E. I. C. Ohlund, E. Schlangen, and S. Erik Offerman, “The kinetics of softening and microstructure evolution of martensite in Fe–C–Mn steel during tempering at 300°C,” *Materials Science and Engineering: A*, vol. 560, pp. 351–357, Jan. 2013.

[18] G. B. Olson and M. Cohen, “Early stages of aging and tempering of ferrous martensites,” *Metall. Trans. A*, vol. 14, no. 6, pp. 1057–1065, Jun. 1983.

[19] G. Krauss, “Tempering of Lath Martensite in Low and Medium Carbon Steels: Assessment and Challenges,” *Steel Res. Int.*, vol. 88, no. 10, p. 1700038, Oct. 2017.

[20] Y.J. Won, Y.J. Kwon, H.K. Moon, S.K. Park, H. Kwon, and K.S. Cho, “Secondary hardening behavior in ausformed martensitic alloys with different Co content,” *Physica B Condens. Matter*, Nov. 2017.

[21] C. J. Kuehmann, G. B. Olson, and H.J. Jou, “Nanocarbide precipitation strengthened ultrahigh-strength, corrosion resistant, structural steels,” 7160399, 09-Jan-2007.

[22] M. Amirkamali and M. Aghaie-Khafri, “The Effects of Ausforming on the Precipitating Process and Mechanical Properties of 17-4PH Stainless Steel,” in *ASME 2010 10th Biennial Conference on Engineering Systems Design and Analysis*, 2010, pp. 711–716.

[23] H. Beladi, G. L. Kelly, and P. D. Hodgson, “Microstructural evolution of ultrafine grained structure in plain carbon steels through single pass rolling,” *Materials Science and Technology: MST; London*, vol. 20, no. 12, pp. 1538–1544, Dec. 2004.

[24] G. Zhu and S. V. Subramanian, “Ultra-fine grain size control and mixed grains elimination in industrial multi-pass rolling processing,” *Materials Science and Engineering: A*, vol. 426, no. 1, pp. 235–239, Jun. 2006.

[25] A. Belyakov, K. Tsuzaki, H. Miura, and T. Sakai, “Effect of initial microstructures on grain refinement in a stainless steel by large strain deformation,” *Acta Mater.*, vol. 51, no. 3, pp. 847–861, Feb. 2003.

[26] H. S. Sim, K. S. Cho, K. B. Lee, H. R. Yang, and H. Kwon, “Mechanical properties in ultrahigh strength secondary hardening steels bearing Co and Ni,” in *Materials science forum*, 2007, vol. 539, pp. 4417–4421.

[27] K. S. Cho, S. S. Park, H. K. Kim, Y. B. Song, and H. Kwon, “Precipitation Kinetics of M2C Carbide in Severely Ausformed 13Co-8Ni Secondary Hardening Steels,” *Metall. Mater. Trans. A*, vol. 46, no. 4, pp. 1535–1543, Apr. 2015.

[28] A. J. Clarke *et al.*, “Atomic and nanoscale chemical and structural changes in quenched and tempered 4340 steel,” *Acta Mater.*, vol. 77, pp. 17–27, Sep. 2014.